Kathleen G. Cleary and Zhengyu Xia contributed equally to this work.

Key Points:
- Widespread meter-scale peat patches found on Arctic tundra may represent the initial stage of new peatland formation
- Paleoecological data indicate that climate cooling and warming led to the initiation and rapid growth of peat patches, respectively
- We might have underestimated the potential role of future peatland-rich landscape on pan-Arctic carbon balance

Correspondence to:
Z. Xia and Z. Yu,
zhyxia@hotmail.com;
yuzc315@nenu.edu.cn

The Growth and Carbon Sink of Tundra Peat Patches in Arctic Alaska

Kathleen G. Cleary[1] [ID]**, Zhengyu Xia[1,2]** [ID]**, and Zicheng Yu[1,2,3]** [ID]

[1]Department of Earth and Environmental Sciences, Lehigh University, Bethlehem, PA, USA, [2]Key Laboratory of Geographical Process and Ecological Security in Changbai Mountains, Ministry of Education, School of Geographical Sciences, Northeast Normal University, Changchun, China, [3]State Key Laboratory of Black Soil Conservation and Utilization, Northeast Institute of Geography and Agroecology, Chinese Academy of Sciences, Changchun, China

Abstract Recent amplified climate warming in the Arctic has caused profound changes in terrestrial ecosystems, with the potential for strong feedback on climate change. Arctic tundra landscapes have developed patchy and thin organic soil (peat) layers at the surface that may continue to grow into mature peatlands and become a larger carbon sink under future warming. Here we use paleoecological analyses of multiple soil and peat cores collected from the North Slope of Alaska to document and understand the formation and development histories of tundra peat patches and permafrost peatlands. We find a consistent peat development sequence for peat patches, first from mineral soils to sedge peat during the Little Ice Age, and then to *Sphagnum* peat during the recent warming with high carbon accumulation rates. These findings suggest that climate cooling is likely critical for the initial peat buildup on tundra soils due to reduced decomposition, whereas climate warming triggers the regime shift into an increased abundance of *Sphagnum* mosses that are likely central to enhancing their carbon sink capacity. Additionally, peat patches become similar to permafrost peatlands in the vicinity in terms of ecosystem processes and carbon dynamics, and therefore may have developed the same ecohydrological feedback system to maintain their long-term stability. This study implies that the potential future expansion of peat patches into peatlands may strongly alter the carbon balance of Arctic tundra, supporting the new United Nations Environment Programme's report that calls for incorporating widespread shallow peat into understanding the peatland–carbon–climate nexus.

Plain Language Summary The ongoing trend of global warming has the fastest rate in the Arctic and has caused rapid and widespread environmental changes in the Arctic tundra. A major concern is the warming-induced permafrost thaw that may destabilize the rich soil-carbon pools underground, providing positive feedback to further accelerate warming. However, warming may also induce northward expansion of northern peatlands that function as persistent carbon sinks over millennia, just like how northern peatlands colonized boreal and sub-Arctic landscapes during and after deglacial warming 14,000~8,000 years ago. If true, new peatland formation may provide negative feedback to mitigate warming. This study focuses on patchy and thin peat layers found on Alaska's tundra and uses paleoecological analyses to understand their histories on the landscape. We find that these peat patches were formed during the cold Little Ice Age, but recent climate warming triggered a shift into dominance of *Sphagnum* mosses, the major peat-forming species for northern peatlands. By comparing with permafrost peatlands nearby, we present multiple lines of evidence to argue that tundra peat patches may be transformed into new Arctic peatlands with important carbon-cycle consequences and recommend future research to further understand such processes with new observational data, laboratory experiments, and model simulations.

1. Introduction

As one of the world's major biomes, the Arctic tundra contains a large portion of global soil carbon (C) stocks within the active layer and deeper permafrost (Hugelius et al., 2014; Ping et al., 2008; Schuur et al., 2015). In recent decades, the Arctic has warmed several times faster than the global average due to a range of mechanisms such as ice-albedo-temperature feedback (Rantanen et al., 2022; Walsh, 2014), resulting in widespread ecological changes on the tundra landscape including shrub expansion (Myers-Smith et al., 2011; Tape et al., 2006), earlier and enhanced vegetation growth known as "Arctic greening" (Jia et al., 2003; Kim et al., 2021; Myers-Smith et al., 2020), permafrost thaw (Hugelius et al., 2020; Schuur et al., 2009; Turetsky et al., 2020), and wildfire events (Hu et al., 2015; Mack et al., 2011; Scholten et al., 2022). These changes may induce other climate

feedback through their impacts on ecosystem C cycling (Bouskill et al., 2020; Bradford et al., 2016; Luo, 2007). However, the response of tundra ecosystems to future climate change and the fate of their large soil C stocks are unclear, in particular for belowground processes and associated C budgets (Bouskill et al., 2020; Sistla et al., 2013). Using different methods and data sets, previous studies of ecosystem C fluxes have suggested that Arctic tundra ecosystems likely function as CO_2 sources, sinks, or are almost CO_2-neutral at present (Commane et al., 2017; Euskirchen et al., 2017; McGuire et al., 2012; Ramage et al., 2024; Virkkala et al., 2021). Earth system models also have limited skills in representing modern C stocks and fluxes of Arctic tundra (Commane et al., 2017; Todd-Brown et al., 2013) and are highly uncertain in predicting their future changes in C cycling (Natali et al., 2019; Qian et al., 2010; Tao et al., 2021).

Arctic tundra has peaty soils or a distinct surface organic-rich layer that can be 5–20 cm thick (Goryachkin et al., 1999; Juselius et al., 2022; Walker et al., 1989, 2005). This layer often contains >30% organic matter (OM), roughly equivalent to >15% organic C (Bockheim et al., 1999; Klaminder et al., 2009), a common requirement for being defined as peat, but traditionally cannot be defined as peatlands because the peat layer is patchy (meters in extent) and too thin (<30 cm) (Joosten & Clarke, 2002; Rydin & Jeglum, 2013). The newly published Global Peatlands Assessment by the United Nations Environment Programme (UNEP) suggests that a shallower threshold of 10 cm for defining peatlands "might be more appropriate in order to account for peatlands' contribution to climate" and from conservation consideration (UNEP, 2022). Doing so will dramatically increase the global peatland area, in particular in the Arctic. For example, the peatland area will almost triple in Russia (UNEP, 2022). Although the UNEP report has recognized the importance of widespread shallow peat, little is known about the fate of peat patches—whether they will continue to grow into mature peatlands and function as persistent C sinks in the future. Tundra peat patches are not comparable to today's northern peatlands in the size of C stocks, but these two peat-forming ecosystems share apparent similarities—both require a persistent C imbalance with plant production greater than ecosystem respiration and both may have a ground cover of *Sphagnum* mosses (peat mosses) (Harden et al., 1992; Walker et al., 1989, 2005), an ecosystem engineer that favors peat accumulation through modifying their ambient environments (Clymo & Hayward, 1982; Rydin & Jeglum, 2013; van Breemen, 1995). The difference is that tundra peat patches are moist (due to cold climate and permafrost) but not waterlogged as for northern peatlands. However, and importantly, peat patches develop widely on tundra landscapes and do not appear to rely on particular terrain features such as polygons or local depressions, whereas intact waterlogged peatlands in Arctic tundra are associated with such often due to the influence of permafrost that alters local drainage patterns (Sim et al., 2019; Tarnocai & Stolbovoy, 2006; Treat et al., 2016; Zoltai & Tarnocai, 1975).

Northern peatlands, mostly found in warmer boreal and sub-Arctic regions further south, are remarkable terrestrial C sinks where organic C has accumulated under waterlogged conditions over millennia or even longer (Yu, 2012; Yu et al., 2009) (Figure 1b). The spatiotemporal changes of northern peatlands, including their inceptions, accumulations, and expansions, play a major role in the global C cycle and have affected atmospheric greenhouse-gas concentrations through time (MacDonald et al., 2006; Stocker et al., 2017; Yu et al., 2010, 2011). Although peatland development and carbon accumulation are controlled by a diversity of internal and external drivers as revealed in many site-specific studies (Klein et al., 2013; Payne et al., 2016; Piilo et al., 2020), global data syntheses indicated that longer and warmer growing seasons are crucial to promote peatland inception and growth, while the factor of increased effective moisture is secondary and regionally important (Charman et al., 2013; MacDonald et al., 2006; Morris et al., 2018; Treat et al., 2019; Yu et al., 2009, 2010). As the Arctic becomes warmer (and wetter) and the trend continues (McCrystall et al., 2021; Rantanen et al., 2022), the tundra landscape will, in the future, expand its climate space to become more like current boreal and sub-Arctic regions that have supported the development of extensive peatlands during the Holocene (Yu et al., 2009) (Figure 1a). Based on the climate space theory, it is possible that amplified climate warming may turn, or is turning, Arctic tundra into an even more peatland-rich landscape, with widespread peat patches that may serve as the initial stage of new peatland formation. Although some studies highlight that climate warming may result in the loss of suitable climate space and the shrink of C sinks for peatlands in relatively lower latitudes (Fewster et al., 2022; Gallego-Sala et al., 2018), recent coupled model simulations with peatland nodules do support the potential future trajectory of poleward peatland migration (Chaudhary et al., 2020; Müller & Joos, 2021; Qiu et al., 2020). However, we do not fully understand how this migration may occur, and more specifically, the connections in ecosystem functions and processes between shallow peat patches and mature peatlands due to the paucity of records that can reveal their genesis and evolution histories.
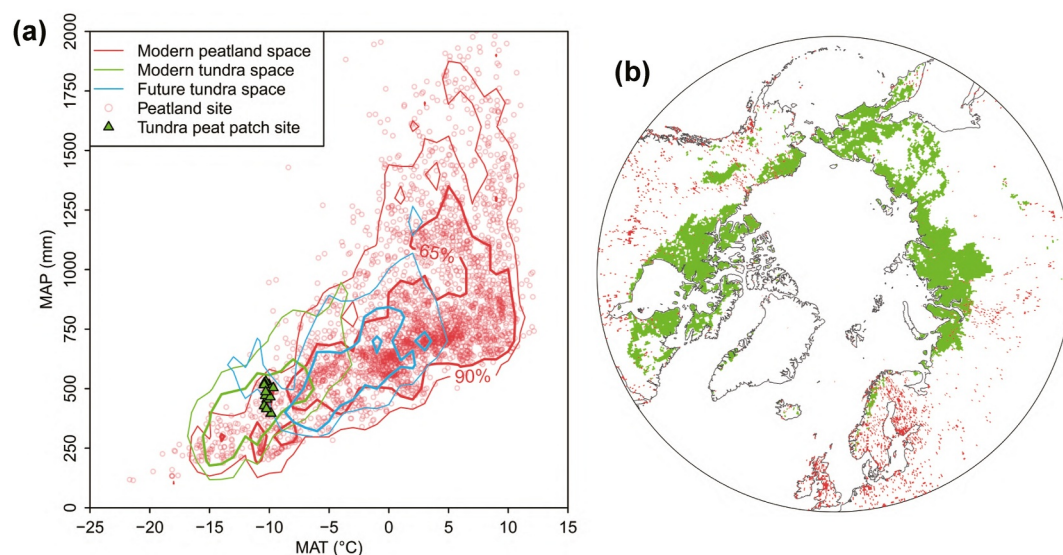
Figure 1. The climate space and latitudinal distribution of Arctic tundra and northern peatlands. (a) The probability climate space (65% and 90% probability in thick and thin lines, respectively) of mean annual temperature (MAT) and precipitation (MAP) for modern peatlands north of 45°N (red lines) and for modern and future Arctic tundra (green and blue lines, respectively). The peatland climate space is based on all $0.25° \times 0.25°$ grids (individually plotted as red open circles) that contain peat cores in the observational database by Hugelius et al. (2020). The Arctic tundra climate space is based on all $0.25° \times 0.25°$ grids north of 45°N classified as tundra in low-vegetation cover (with low vegetation cover >80%) from the ERA5 reanalysis (Hersbach et al., 2020). Modern climate data are from the ERA5 reanalysis (during the period 1981–2010 CE) (Hersbach et al., 2020). Future climate data for the modern Arctic tundra region are CMIP5 multi-model ensemble means during the period 2080–2099 CE under RCP8.5 scenario (Taylor et al., 2012). Also shown are modern climate conditions at locations of tundra peat patches (green triangles) discovered by the authors (see Figure 2a for geographical locations). (b) A north polar view of the spatial distribution of Arctic tundra (green grids) and peatland (red grids, overlaid on tundra where overlapped) that are used to derive their climate spaces.

In this study, we fill this fundamental knowledge gap by using multi-core and multi-proxy paleo-records from the North Slope of Alaska (NSA) to document the formation and development histories of tundra peat patches and permafrost peatlands along with a reconstruction of environmental and ecological changes in this region. This study is, to our knowledge, one of a few that can examine the peat accumulation dynamics from shallow non-peatland archives, a topic of current concern for the UNEP and related policy makers (Juselius et al., 2022; UNEP, 2022; Wilkinson et al., 2020). Our objectives are to investigate (a) when peat patches emerged on tundra mineral soils and how they changed over time; (b) what factors control the growth and C sink capacity of peat patches; and (c) what roles these peat patches may play in the future C balance of the Arctic. For each objective, we specifically hypothesize that (a) peat patches initiated and accumulated most carbon during past warm periods; (b) climate is the main factor controlling the growth and C sink capacity of peat patches; and (c) peat patches show high similarities with peatlands in ecosystem functions and processes and will become important C sinks in Arctic tundra.

2. Materials and Methods

2.1. Study Sites and Samples

This study investigates two sites in the northern foothills of the Brooks Range on NSA (Figures 2a and 2b): the Upper Imnavait Creek (UIC) tussock tundra site (68.60°N, 149.30°W) and the permafrost-affected Kuparuk River Peatland (KRP) site (68.96°N, 149.67°W). UIC is located next to Imnavait Creek, a tributary of Kuparuk River, and is approximately 12 km east of Toolik Lake (adjacent to the Toolik Field Station). KRP is approximately 40 km north of Toolik Lake.

In the Toolik Lake area, the mean annual temperature is −8.5°C, and the mean summer (June–August) temperature is 9°C (Daniels et al., 2017). Only summer months are above freezing. The mean annual precipitation exceeds 300 mm, with ~60% falling as rain during the summer months (Daniels et al., 2017). The area is covered
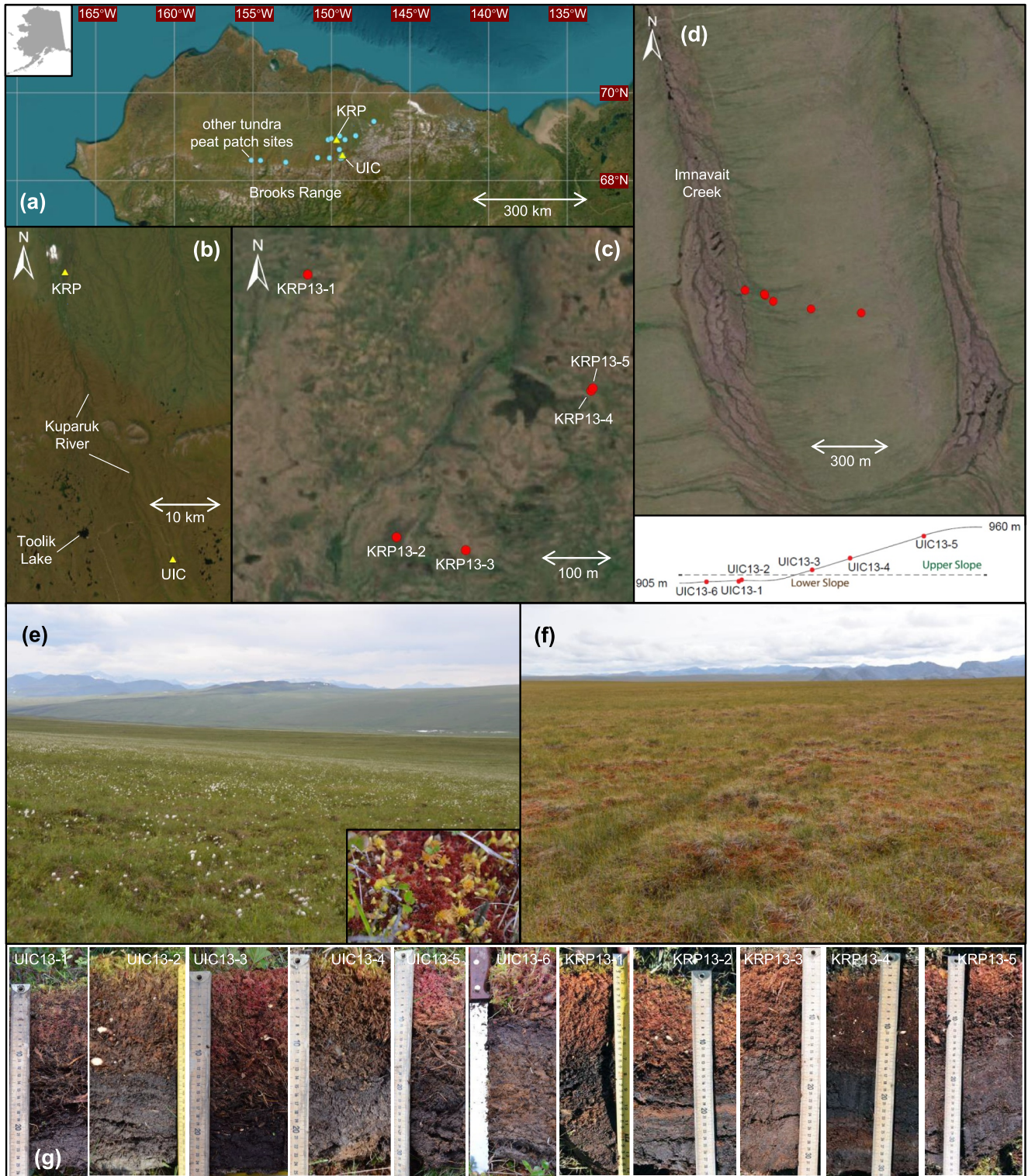
Figure 2. Maps and photos showing the locations and settings of study sites on the North Slope of Alaska (NSA). (a) Locations of the Upper Imnavait Creek (UIC) and the Kuparuk River Peatland (KRP) (yellow triangles) along with other tundra peat patch sites (cyan dots) discovered during a fieldwork campaign in summer 2019. (b) Areas of UIC and KRP relative to Toolik Lake. (c) Locations of KRP cores. (d) Locations of UIC cores and their positions along a hillslope transect. (e) Field view of UIC and discovered *Sphagnum*-dominated peat patches (dominated by *Sphagnum rubellum*). (f) *Sphagnum*-dominated peat patches at another typical site on the NSA. (g) Soil/peat core photographs.

Table 1
Main Information About Collected Cores

Core ID	Latitude	Longitude	Elevation (m asl)	Core length (cm)	Dominating *Sphagnum* species
UIC13-1	68°36′02.4″N	149°18′18.0″W	908	44.3	*S. girgensohni*
UIC13-2	68°36′02.6″N	149°18′18.3″W	908	25	*S. girgensohni*
UIC13-3	68°36′01.7″N	149°18′15.1″W	916	24	*S. rubellum*
UIC13-4	68°36′00.7″N	149°18′01.9″W	927	26	*S. rubellum*
UIC13-5	68°36′00.2″N	149°17′44.2″W	950	26	*S. rubellum*
UIC13-6	68°36′03.1″N	149°18′25.1″W	906	29	*S. rubellum, S. girgensohni*
KRP13-1	68°57′34.8″N	149°40′34.8″W	417	35	*Sphagnum* spp.
KRP13-2	68°57′22.8″N	149°40′23.5″W	403	52	*Sphagnum* spp.
KRP13-3	68°57′22.2″N	149°40′14.7″W	427	31	*Sphagnum* spp.
KRP13-4	68°57′29.5″N	149°39′58.7″W	422	31	*Sphagnum* spp.
KRP13-5	68°57′29.6″N	149°39′58.5″W	423	32	*Sphagnum* spp.

by snow for the rest of the year. The Kuparuk watershed region is mantled by mid-Pleistocene-age Sagavanirktok glacial deposits, with a gently sloping surface containing abundant colluvial and organic deposits (Hamilton, 1986). NSA is in the continuous permafrost zone. In the Toolik Lake area, the permafrost is ∼200 m thick and only partially thaws during the summer (Huryn & Hobbie, 2012). The active layer is on average ∼36 cm deep and often moist (Walker & Walker, 1996). There, tussock sedge tundra is the most common vegetation class (Walker et al., 1989, 2005). Specifically, the plant community at acidic uplands of UIC is dominated by tussock sedges ("cotton grass," *Eriophorum vaginatum*) and reddish *Sphagnum rubellum* (Figure 2e). Other important species include dwarf shrubs (*Betula nana*, *Salix planifolia*), non-tussock sedges (*Carex bigelowii*), orangish *Sphagnum lenense* (upper hillslope), and greenish *Sphagnum girgensohnii* (lower hillslope and floodplain). Notably, *S. rubellum* and *S. lenense* are acidic, nutrient-poor species, while *S. girgensohnii* is a poor fen (weakly minerotrophic) species (Kuptsova & Chakov, 2022; Rydin & Jeglum, 2013).

During the fieldwork campaign in summer 2013, six soil cores were collected at UIC from *Sphagnum*-dominated peat patches along a hillslope (∼50 m elevation gradient) transect, and five peat cores were collected at KRP (Figures 2c and 2d; Table 1). These cores were all collected at locations free of obvious hydrological and topographic variations to minimize potential local influences on peat accumulation. UIC is the primary study site on peat patches, while KRP is used as a supporting peatland site for comparison. These cores were retrieved with a combination of a large serrated knife, hand-operated peat corer, and gasoline-powered permafrost corer. Back in the laboratory, cores were cut into 1-cm slices and subsampled for a suite of paleoecological analyses, including radiocarbon (^{14}C) dating, loss-on-ignition (LOI), plant macrofossils, pollen assemblages, bulk peat C and nitrogen (N) abundances and isotopic compositions, *Sphagnum* stem cellulose C and oxygen (O) isotopic compositions (see a summary of analyses in Table 2). These analyses were mainly conducted for four master cores: UIC13-1, UIC13-2, UIC13-3, and KRP13-2 (Figure 2g).

2.2. Laboratory Analysis

Physical properties (OM content and OM bulk density) of cores were analyzed at 1-cm intervals following a standard procedure. Subsamples (1 cm^3) were weighed, dried in the oven at 80°C overnight, weighed again, combusted at 550°C for 2 hrs, and weighed again to determine the mass loss as an estimate of the OM content.

Plant macrofossils were analyzed at 1-cm intervals for cores UIC13-1, UIC13-2, UIC13-3, and KRP13-2. Subsamples (1 cm^3) were gently washed with deionized water and sieved through a 125-μm mesh to concentrate macrofossils, which were then identified under a stereo microscope. The relative abundance of each macrofossil type or unidentified organic matter was estimated as the percentage by volume. A stratigraphically constrained cluster analysis (CONISS) was used to determine the zonation of macrofossil assemblages using the Tilia program (Grimm, 1987).

Table 2
Summary of Analyses Conducted and Apparent C Accumulation Rates (aCAR) for Sedge and Sphagnum Peat Intervals (NA = not Available)

Core ID	LOI	Macrofossil	Pollen	Bulk C/N, δ^{13}C, and δ^{15}N	*Sphagnum* cellulose δ^{13}C and δ^{18}O	^{14}C dating	Age-depth model	Sedge peat aCAR (gC/m^2/yr)	*Sphagnum* peat aCAR (gC/m^2/yr)
UIC13-1	√	√		√		√	√	28	75[a]
UIC13-2	√	√			√	√	√	14	72
UIC13-3	√	√	√	√	√	√	√	5	40
UIC13-4	√					√		9	119
UIC13-5	√					√		NA	50
UIC13-6	√					√		17	66
KRP13-1	√					√		17	130
KRP13-2	√	√	√		√	√	√	6	22[a]
KRP13-3						√		NA	NA
KRP13-4	√							NA	NA
KRP13-5						√		NA	NA

[a]*Sphagnum* onset ages were determined based on the interpolation from the age-depth model.

Fossil pollens were analyzed at 1-cm intervals for cores UIC13-3 and KRP13-2. Subsamples (1 cm^3) were processed following a modified standard acetolysis procedure, including sieving and treatments of HCl, KOH, HF, and acetolysis. Pollen grains from the samples were identified and counted to a sum of at least 100 grains under a compound microscope. A stratigraphically constrained cluster analysis (CONISS) was similarly used to determine the zonation of pollen assemblages using the Tilia program (Grimm, 1987).

Bulk peat C and N elemental concentrations and their isotopic compositions were measured at 1-cm intervals for cores UIC13-1 and UIC13-3. Subsamples (1 cm^3) were freeze-dried and then homogenized. *Sphagnum* moss cellulose C and O isotopic compositions were measured at 1-cm intervals (that contain sufficient *Sphagnum* macrofossils) for cores UIC13-2, UIC13-3, and KRP13-2. *Sphagnum* moss stem fragments were hand-picked with branches removed from subsamples (2–4 cm^3), extracted for cellulose following the established alkaline-bleaching method (Loader et al., 1997), homogenized, and freeze-dried (Xia et al., 2018). Prepared samples of sufficient amount were enclosed into capsules and analyzed with the well-established elemental analyzer-mass spectrometer coupled systems at the Stable Isotope Facility at the University of California, Davis, USA. Following the routine, results of isotope ratio measurements were calibrated and reported as δ notations (in per mil) referenced to Vienna Pee Dee Belemnite for δ^{13}C, air for δ^{15}N, and Vienna Standard Mean Ocean Water for δ^{18}O. The reported long-term standard deviation for each analysis is 0.2%, 0.3%, and 0.3%, respectively.

Peat ^{14}C ages were measured at selected levels to determine the timing of peat inception and *Sphagnum* onset. For basal peat ages, dating material was composed of macrofossils of non-aquatic taxa (Quik et al., 2022), or, if the sample lacked identifiable macrofossils, root-free bulk peat materials were used. For *Sphagnum* onset ages, dating material was composed of the first-appeared major *Sphagnum* peat horizon in each core. Additional dating samples were taken from cores to establish age-depth models for the discussion of environmental change and C accumulation records. These materials were washed with deionized water and dried in the oven. Samples were pretreated and dated at the Keck AMS Carbon Cycle Lab at the University of California, Irvine, USA. Results were calibrated based on the IntCal20 and Bomb21NH1 calibration data sets for pre- and post-bomb ^{14}C dates, respectively (Hua et al., 2022; Reimer et al., 2020). Simple age-depth models were developed for cores UIC13-1, UIC13-2, and UIC13-3 using the linear interpolation method and for core KRP13-2 using the smooth spline method on the CLAM program (Blaauw, 2010). The advantages of linear interpolation for detecting potential abrupt changes in accumulation rates have been previously discussed in Yu et al. (2014). Importantly, we used multiple post-bomb ^{14}C dates before and after the atmospheric ^{14}C peak of 1965 CE to constrain the chronology of the most recent peat accumulation. Some ^{210}Pb dates were obtained for core UIC13-1 but were not considered here due to possible mobility downcore (see Cleary, 2015). The apparent C accumulation rates (aCAR) were calculated for some cores using measured C contents if available or assuming the mean value of available data, with age-depth models or between dated intervals.

3. Results

Our multi-proxy data reveal the genesis and evolution of multiple tundra peat patches, the history of a permafrost-affected peatland, and the history of Arctic tundra vegetation and climate on NSA.

Loss-on-ignition data (Figure 3a and Figure S1 in Supporting Information S1): LOI data provide a major overview of soil and peat stratigraphy. The OM content is substantially low at the bottom mineral-soil section of UIC cores (except UIC13-5). The higher OM content further up indicates the inception of peat accumulation over mineral soils. The OM bulk density has a decreasing trend toward the top, representative of the shift from highly decomposed to poorly decomposed peat. For KRP cores, OM content and density profiles show more than one mineral-rich layer, possibly related to permafrost interactions, and generally highly decomposed peat in the lower section.

Macrofossil data (Figures 3c and 4): Plant macrofossil data reflect the changes in the dominant vegetation that composes the peat. For three master UIC cores, macrofossil data show a consistent sequence of organic soil development from mineral soils to sedge peat and then to *Sphagnum* peat. For the master KRP core, there is also a clear transition from sedge peat to *Sphagnum* peat in the upper section, but *Sphagnum* macrofossils are not absent in the lower section.

Pollen data (Figures 3d and 5): Our two pollen records are among very few studies (Gałka et al., 2018) that can provide a continuous, long-term perspective on the recent warming-driven shrub expansion on the Alaskan tundra, previously only documented by short-term vegetation plots, remote sensing products, and repeat photographs (Tape et al., 2006). Both UIC and KRP sites show a sequence of increasing shrub pollen proportion from <20% at the bottom to >80% at the top of the core. The decrease in Cyperaceae (sedge family) pollen percentage mainly occurs with the increases in *Betula* and Ericaceae (heath family) pollen percentages. For the UIC site, however, other pollen taxa (*Picea*, *Salix*, *Alnus*) increase at the expense of *Betula* and Ericaceae pollen toward the top of the core. A more detailed analysis of pollen data as a record of ecological changes in tundra ecosystems at local and regional scales is out of scope but can be referred to Cleary (2015) for a brief discussion.

Bulk peat elemental and isotopic data (Figure 3b and Figure S2 in Supporting Information S1): Bulk peat elemental and isotopic values are useful stratigraphical indicators, but they are controlled by multiple factors including botanical compositions, C and N sources, and the degree of decomposition (Broder et al., 2012; Jones et al., 2010; Treat et al., 2016). For cores UIC13-1 and UIC13-3, C and OM contents are linearly correlated; on average core samples contain 46% C in OM. In both cores, the C/N value increases from <20 to >40 while the $\delta^{13}C$ and $\delta^{15}N$ values decrease by >4% and >7%, respectively, toward the top. Based on their values in modern plants (Shaver & Yano, 2016) and corresponding shifts in macrofossil assemblages, we suggest that these supporting data mainly reflect the stratigraphy in botanical compositions of OM from sedge peat to *Sphagnum* peat and, secondly, the known "Suess effect" (due to anthropogenic CO_2 emissions from fossil fuel burning) on $\delta^{13}C$.

Cellulose isotopic data (Figure 3d): *Sphagnum* cellulose $\delta^{13}C$ and $\delta^{18}O$ data are independent climate proxies in peat-based paleoenvironmental reconstructions (Fu et al., 2022; Kaislahti Tillman et al., 2013; Xia et al., 2018). From the current understanding of these two proxies (Xia et al., 2018), cellulose $\delta^{18}O$ data mainly reflect changes in source water (precipitation) $\delta^{18}O$ (Daley et al., 2010). In this high-latitude region, precipitation $\delta^{18}O$ is positively correlated with air temperature following the "temperature effect" (Daniels et al., 2017; Dansgaard, 1964). Cellulose $\delta^{13}C$ data, after accounting for the "Suess effect," mainly reflect changes in *Sphagnum* wetness (Xia, Zheng, et al., 2020). For three master cores from both UIC and KRP sites, the *Sphagnum* cellulose $\delta^{13}C$ and $\delta^{18}O$ values generally shift lower and higher, respectively, toward the top but their trends appear to be reversed in a few topmost core samples. The consistent—albeit not statistically significant—positive correlations between paired $\delta^{18}O$ and "Suess effect"-corrected $\Delta^{13}C$ (the difference between $\delta^{13}C$ of atmospheric CO_2 and plant cellulose) in all three cores potentially indicate that higher temperature and lower *Sphagnum* wetness are closely coupled (Figure S4 in Supporting Information S1).

Radiocarbon data (Figure 6a; Table S1 in Supporting Information S1): Radiocarbon-dated peat and soil cores and multi-proxy data allow us to unravel the timing and C-cycle consequence of the past transformation of peat-forming ecosystems on the tundra biome. At UIC, the initiation of sedge peat over mineral soils occurred during 680–330 cal. yr BP ("Present" is 1950 CE). The onset of *Sphagnum* over sedge peat occurred at post-bomb (post-1950 CE) dates or as early as 270 cal. yr BP. Both sedge peat initiations and *Sphagnum* onsets occurred earlier on upper hillslope positions. At KRP, the master core KRP13-2 has a basal age of about 4,000 cal. yr BP
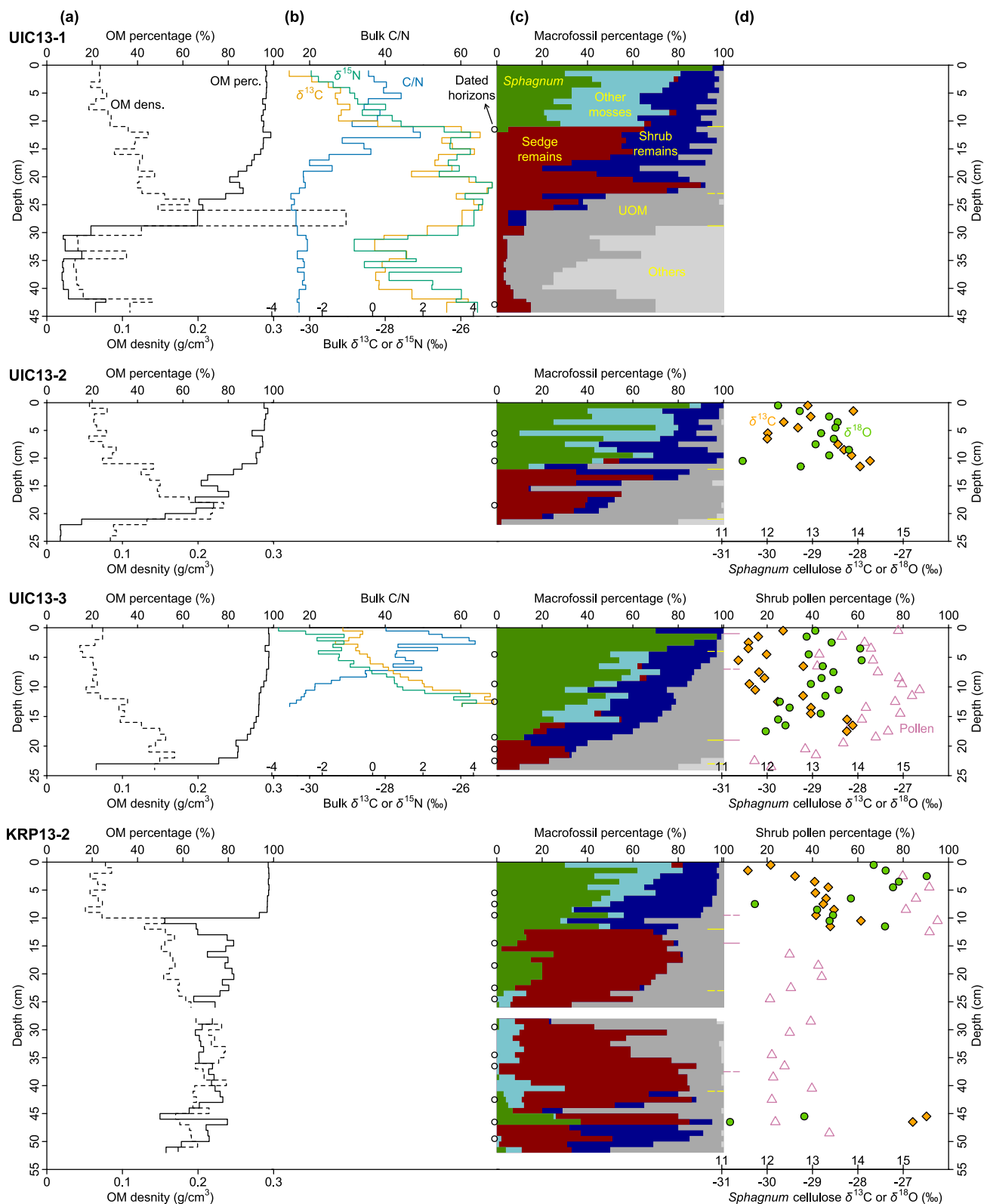
Figure 3.

and a possible hiatus during 2,500–1,200 cal. yr BP (Figure S3 in Supporting Information S1), after which the newest sedge peat re-initiation occurred. For other KRP cores, only younger bounds of sedge peat re-initiation ages can be determined (as we are unsure about whether coring had reached the basal peat layer or was stopped by permafrost) and are as old as 1,000 cal. yr BP. The *Sphagnum* onsets occurred more often at pre-bomb dates as early as 280 cal. yr BP.

Apparent C accumulation rates (Figure 6b; Table 2): The aCAR data from peat cores are often analyzed to reflect changes in peatland C sink capacity over time (Magnan et al., 2022; Swindles et al., 2015; Xia, Oppedal, et al., 2020), but they do not directly represent their C balance (Young et al., 2019, 2021). The aCAR from cores UIC13-3 and KRP13-2 based on their age-depth models (Figure S3 in Supporting Information S1) show large increases from sedge peat to *Sphagnum* peat, from ∼5 to ∼40 gC/yr/m^2 and from ∼6 to ∼22 gC/yr/m^2, respectively. Other cores also show the same phenomenon based on aCAR between dated intervals, on average from ∼17 to ∼85 gC/yr/m^2. Within *Sphagnum* peat intervals from well-dated cores UIC13-3 and KRP13-2, aCAR further show increases after 1960 CE from ∼25 to ∼131 gC/yr/m^2 and from ∼12 to ∼84 gC/yr/m^2, respectively. These aCAR values are all mean values and have not considered the uncertainties related to ^{14}C chronologies. Notably, core UIC13-3 additionally contains a short interval of increased aCAR at around 1900 CE (equivalent to 50 cal. yr BP), followed by a short interval of decreased aCAR during the period 1950–1970 CE.

4. Discussion

4.1. Peat Initiations on Tussock Tundra During the Little Ice Age

The initiation of patchy sedge peat over inorganic, mineral-rich deposits along the hillslope of UIC tussock tundra occurred within a narrow time window (about 1300–1600 CE)—during the late stage of the gradual, two-millennia-long summer cooling trend in the Arctic (Figures 6a and 6d) (Kaufman et al., 2009; McKay & Kaufman, 2014). This time window corresponds to the well-known Little Ice Age (LIA) of the Northern Hemisphere spanning 1300–1850 CE (IPCC, 2007), which is also well documented by multiple paleoclimate records in Alaska (Calkin, 1988; Hu et al., 2001; Loso, 2009). Previous studies in the same region found much older, deeply buried Holocene-age peat, but their cores were collected from the floodplain peatland of Imnavait Creek (Eisner, 1991; Nichols et al., 2017).

Peat initiation during climate cooling shown in our records differs from the emerging view that global initiations of peatlands were primarily triggered by rising growing-season temperatures that enhance ecosystem productivity (MacDonald et al., 2006; Morris et al., 2018; Yu et al., 2010). Their results, however, relied on statistical analyses between the time series of peat basal ages and low-resolution climate records simulated by a climate model (Morris et al., 2018) or coarse-resolution large-scale synthesis data (MacDonald et al., 2006; Yu et al., 2009). The basal peat chronology used in those studies often lacks the stratigraphic and dating details as reported here.

Net peat accumulation is determined by the balance between the production and decomposition of OM (Rydin & Jeglum, 2013; Yu et al., 2009). Our observations suggest that the preservation of OM via slow decomposition rates—which were driven by cold climates and wet soil conditions under reduced evapotranspiration rates (Clymo, 1984)—is perhaps an important overlooked mechanism for initial peat buildup. We hypothesize that regardless of the rates of litter and OM production, small amounts of peat may be preserved over time if decay rates are sufficiently low. As OM has a lower heat conductivity and higher porosity or water-retention capacity than mineral soils, the occurrence of insulating and saturated peat layers on tundra would further inhibit the heat transfer into the ground, increase the latent heat flux, reduce the water stress-related limitations for tundra vegetation, and inhibit microbial decomposition through permafrost aggradation (Beilman et al., 2001; de Vrese & Brovkin, 2021; Du et al., 2022; Moskal et al., 2001; Runkle et al., 2014). This means that once the initial peat forms, it can self-maintain through the feedback system to promote cooler and wetter microclimate conditions

Figure 3. Summary of palaeoecological and geochemical analyses of four master cores (see Figures 4 and 5 for detailed macrofossil and pollen diagrams). For core KRP13-2, a 2-cm gap occurred between the top monolith section and the bottom permafrost core due to sampling complications. (a) Organic matter (OM) percentage and OM bulk density data. (b) Bulk peat C/N, δ^{13}C, and δ^{15}N data. (c) Macrofossil compositions and zones (yellow lines; dashed ones are boundaries of subzones). "UOM" means unidentified organic matter. Shrub remains include their woody twigs, roots, and leaves. "Others" include mineral particles, charcoal, and insect remains. ^{14}C-dated horizons are shown as open dots on the left. (d) *Sphagnum* cellulose δ^{13}C and δ^{18}O data, and percentages of pollen from shrub taxa (*Betula*, *Salix*, *Alnus*, and Ericaceae) and pollen zones (pink lines).
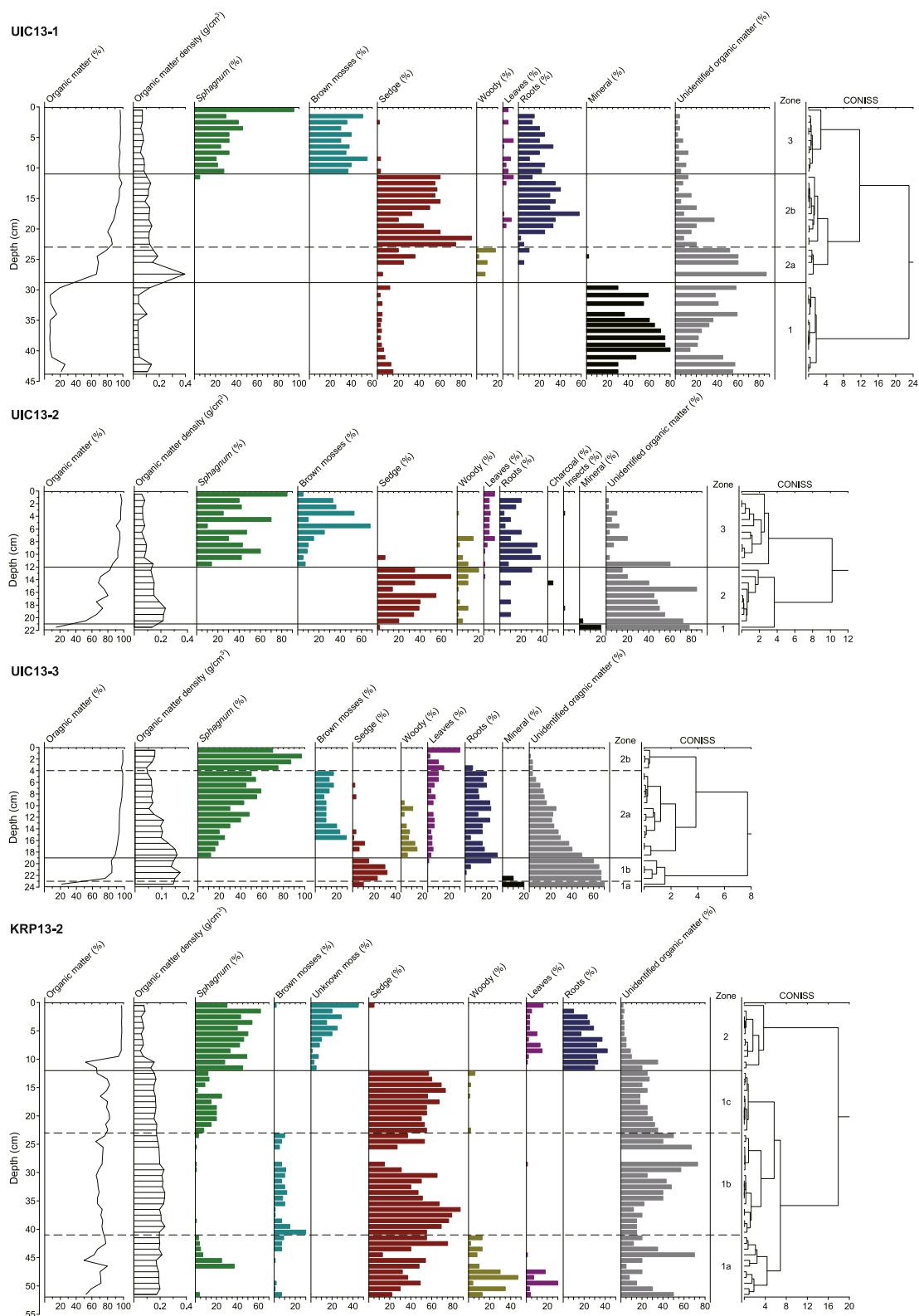
Figure 4. Macrofossil diagrams for cores UIC13-1, UIC13-2, UIC13-3, and KRP13-2, including their CONISS zones. OM percentage and density data are also plotted.
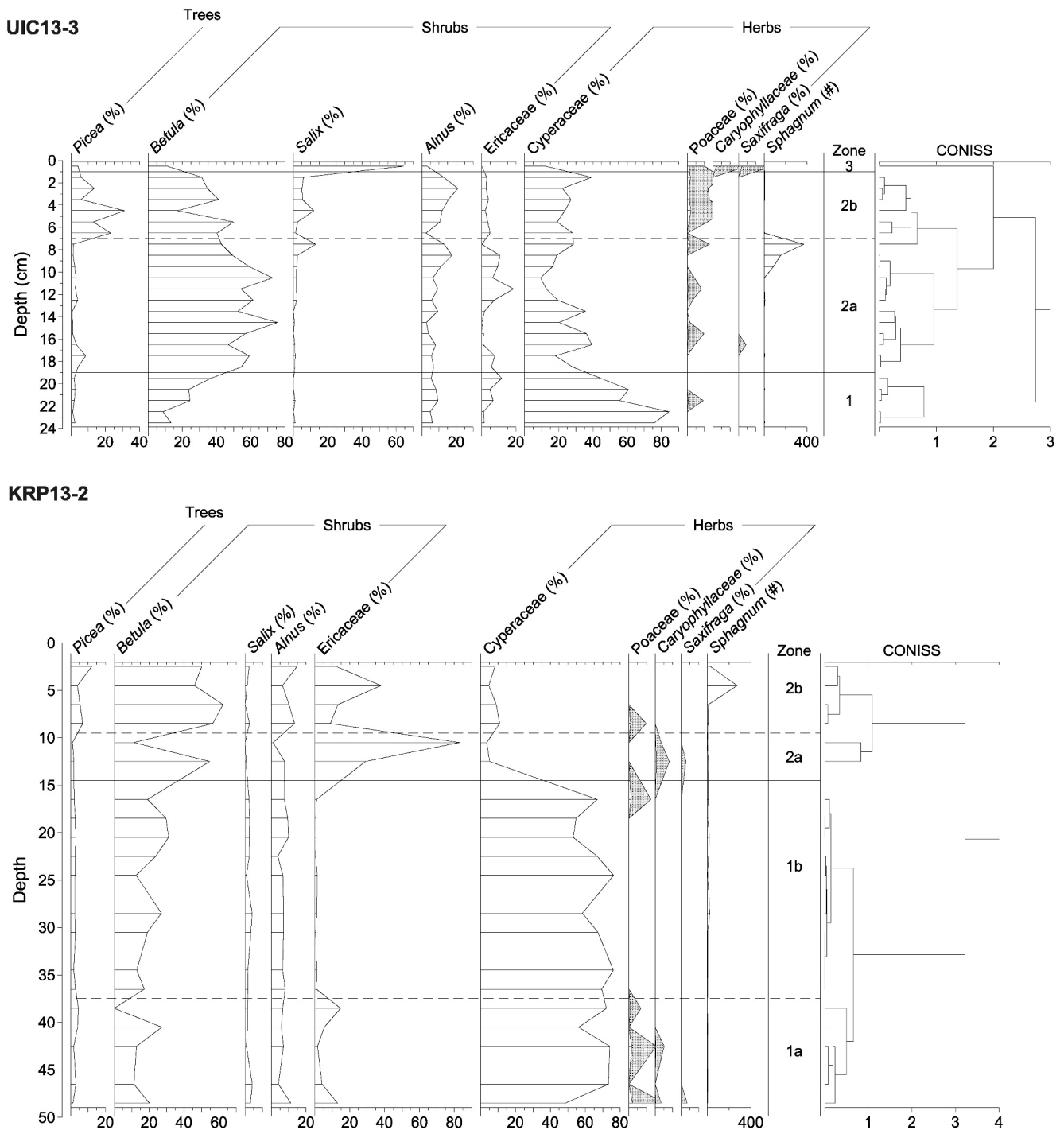
Figure 5. Pollen diagrams for cores UIC13-3 and KRP13-2, including their CONISS zones. Shaded curves show ×10 exaggeration where necessary. Note that indeterminable/unknown pollen grains (not shown) and *Sphagnum* spores were excluded from the pollen sum in calculating the "pollen percentage" in Figure 3d.

favorable to further peat accumulation and stabilization, eventually replacing mineral soils (Belyea, 2009; de Vrese & Brovkin, 2021). If true, this mechanism can be crucial for peat initiation even if only taking several centuries. Furthermore, our data show that peat initiation may occur earlier at upper hillslope positions, not necessarily at the lower, wetter spots (Figure 6a). These findings together provide rare and important insights into a possible pathway for the initial peatland formation worldwide.
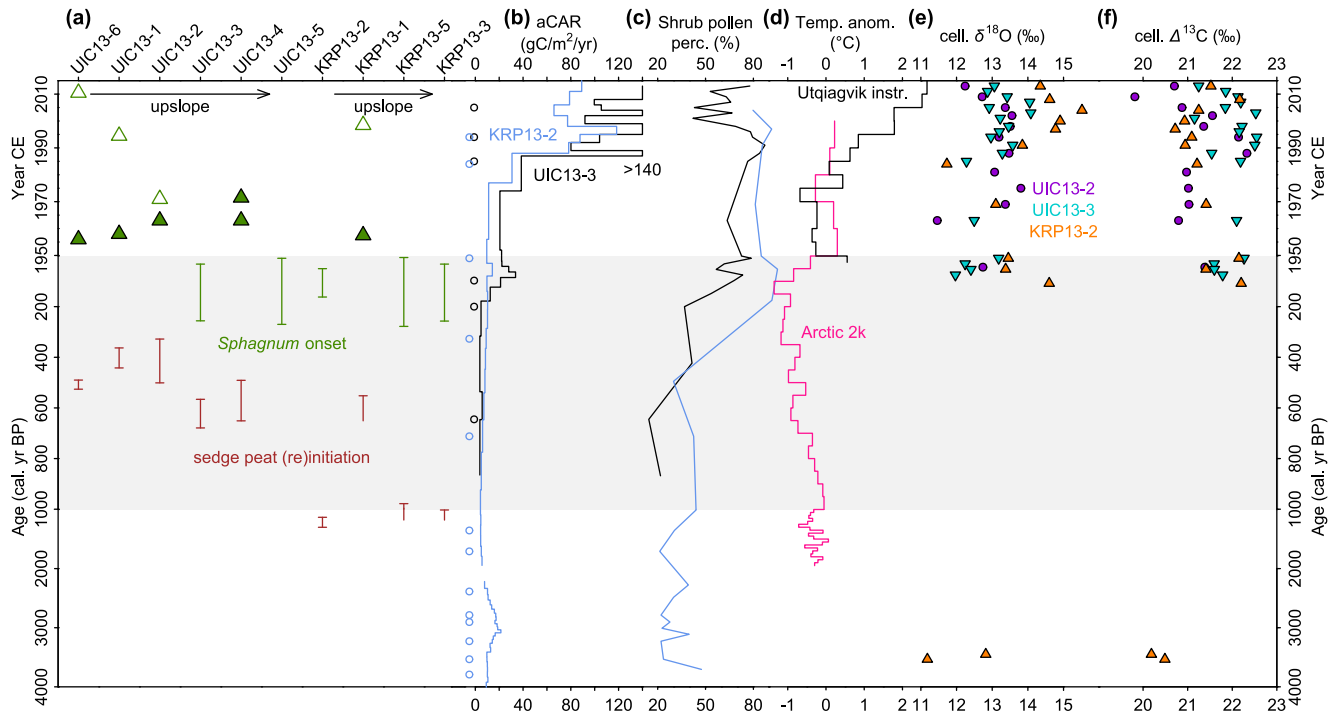
Figure 6. Temporal changes in peat-forming ecosystems and tundra environments. Note the different scales for the post-1950 CE period, during 1,000–0 cal. yr BP, and during 4,000–1,000 cal. yr BP ("Present" is 1950 CE). (a) Chronology of sedge peat (re-)initiations and *Sphagnum* onsets at two study sites labeled at the top. Post-bomb dates are shown in triangles (open triangles are highly unlikely dates; see Table S1 in Supporting Information S1), and pre-bomb dates are shown in 2σ probability bars (some only have younger bounds). (b) Apparent C accumulation rates from cores UIC13-3 and KRP13-2 and their ^{14}C-dated horizons (open dots in corresponding colors). (c) Shrub pollen percentages from the same cores as in panel (b). (d) Temperature anomalies in multiple-year bins relative to the period 1961–1990 CE from the Arctic 2k compilation (McKay & Kaufman, 2014) and instrumental data in Utqiagvik (Barrow), Alaska (NOAA/NCEI, 2024). (e) *Sphagnum* cellulose δ^{18}O records from cores UIC13-2, UIC13-3, and KRP13-2. (f) *Sphagnum* cellulose Δ^{13}C records after correcting for the "Suess effect" following the method by Leuenberger (2007) from the same cores as in panel (e).

At the permafrost-affected peatland site KRP, we speculate that peat initiation occurred as lateral expansion from the location of KRP13-2, eventually forming a continued large peatland complex. The initiation and re-initiation of sedge peat at this site differ in timings from peat patches of UIC (Figure 6a), suggesting potentially different controls between peat patches and permafrost peatlands in regard to their genesis (Figure 7).

4.2. *Sphagnum* Onsets During the Recent Warming Period

The onset of *Sphagnum* peat with almost 100% OM content over highly humified sedge peat (Figure 3a and Figure S1 in Supporting Information S1) occurred in two stages at UIC, with the first stage centered at about 1850 CE for some upper hillslope positions (with a large age uncertainty in pre-bomb dates) and the second stage during 1950–1970 CE (Figure 6a). These two stages are within the anthropogenic warming period characterized by rapid temperature increases (2°C in 200 years) in the Arctic (Kaufman et al., 2009) (Figure 6d). On NSA, the instrumental temperature record at Utqiagvik (Barrow), Alaska, indicates regional cooling during the period 1950–1975 CE (Figure 6d). This cooling reversal during the long-term warming trend is documented by our *Sphagnum* cellulose δ^{18}O records (Figure 6e). Our pollen data also show the warming-driven shrub expansion prior to 1950 CE and a slight reverse afterward (Figure 6c). Still, we caution that *Sphagnum* cellulose δ^{18}O records might be affected by other factors, such as changes in moisture source regions (Gaglioti et al., 2017), or the lengthening of growing seasons. In the latter case, *Sphagnum* mosses under earlier spring onset may utilize an increasing amount of low-δ^{18}O winter precipitation (snowmelt) for carbohydrate biosynthesis (Loisel et al., 2012). The latter mechanism may explain the observed shifts toward lower δ^{18}O after 2000 CE (Figure 6e), but it remains to be rigorously tested. Additionally, although the recent shrub expansion has been documented at another site of the Toolik Lake area (Gałka et al., 2018), all these pollen records from Arctic tundra might be affected by local factors (de Klerk et al., 2009; Gałka et al., 2023; Oswald et al., 2003).
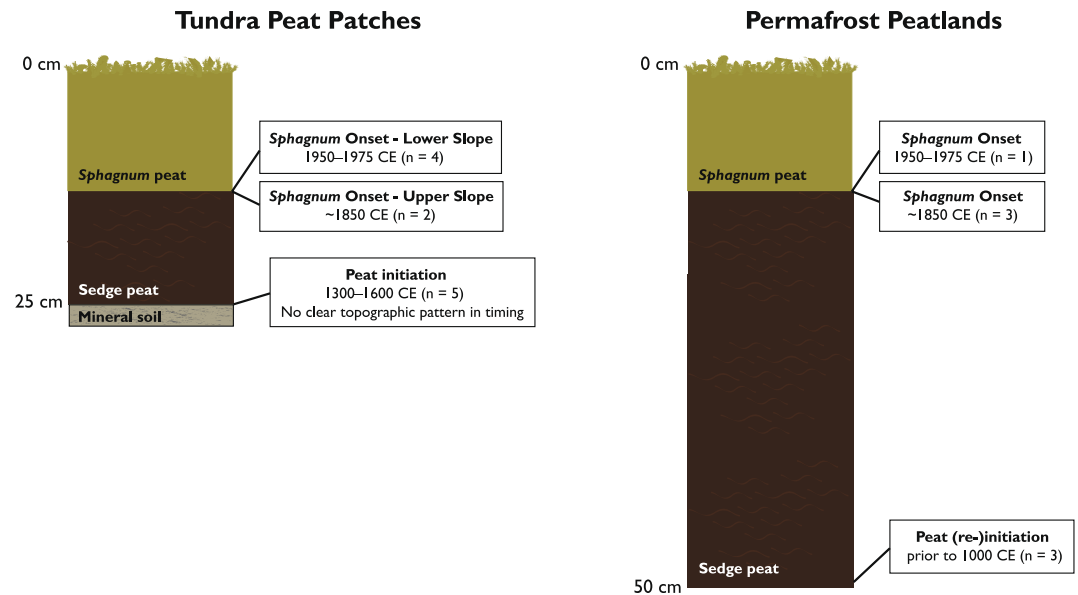
Figure 7. Summary diagram showing the ages of peat initiation and *Sphagnum* onset from soil cores of peat patches at UIC and from peat cores at KRP.

The shift from sedge peat to *Sphagnum* peat is a phenomenon frequently encountered in the evolution of peatlands and preserved in peat stratigraphy, known as the fen-bog transition (FBT) (Barber et al., 2003; Hughes & Barber, 2003; Loisel & Bunsen, 2020; Tahvanainen, 2011; Xia et al., 2024; Yang et al., 2023). FBT describes the abrupt, step-like regime shift from a minerotrophic state under the influence of mineral-rich surface- and ground-water to an ombrotrophic state relying on nutrient-poor precipitation as the water source. Loisel and Yu (2013) have developed a conceptual model for FBT to elaborate on how climate warming can result in the success of dry-tolerant, oligotrophic *Sphagnum* moss species and the transition into a high rate of *Sphagnum* peat accumulation through cascading effects on local hydrology, plant production, and decomposition. This model highlights that the onset of *Sphagnum* peat could be triggered by climate-related allogenic forcing that involves multiple reinforcing feedback loops to sustain or accelerate the autogenic forcing (Loisel & Bunsen, 2020; Loisel & Yu, 2013).

Due to the observed synchronicity of FBT-like changes in peat patches within the time window of the recent warming period with no exception, we suggest that these shifts likely occurred in response to century-long, climate-induced, dramatic shifts in site conditions under anthropogenic warming with a comparable mechanism previously proposed for recent FBT in northern peatlands (Granlund et al., 2022; Loisel & Yu, 2013; Magnan et al., 2022; Piilo et al., 2023). Interestingly, the fact that peat patches in lower positions on the hillslope shifted to *Sphagnum* peat during the decadal-scale cooling period of 1950–1975 CE seems to contradict the warming-induced transition (Figure 6a). However, this contradiction can be reconciled if this decadal-scale cooling was too weak in magnitude and impact compared to the prior centennial-scale warming or did not reverse the continuous warming-induced changes in site conditions that have already reached a critical threshold ready for a regime shift (Belyea, 2009; Loisel & Bunsen, 2020). This interpretation highlights the non-linear features that sometimes characterize peat-forming ecosystems (Belyea, 2009; Belyea & Baird, 2006; Morris et al., 2011). Peat patches dominated by acidic, nutrient-poor species *S. rubellum* and *S. lenense* are nowadays widespread at UIC, particularly in the upper hillslope, indicating a state of climate-driven ombrotrophy for the entire hillslope despite that our paleoecological records only document a few of them.

The recent onsets of *Sphagnum* peat also occurred at our paired permafrost peatland site KRP with comparable timings to that at UIC (Figure 6a). Another permafrost peatland study at the Toolik Lake area showed the same pattern: the *Sphagnum* onsets in their two studied cores occurred in 1850–1900 CE and 1940–1950 CE (Gałka et al., 2018; Taylor et al., 2019). That study also documented the trend toward drier conditions that favor ombrotrophication based on testate amoebae-based water-table depth reconstructions (Taylor et al., 2019). This region-wide, consistent transformation in vegetation structure of different peat-forming ecosystems on the landscape is remarkable and indicates their common controls despite different local hydrology (waterlogged

peatlands vs. non-waterlogged peat patches). However, we also acknowledge that vegetation changes across the Arctic are spatiotemporally heterogeneous and highly sensitive to local substrate or permafrost-related factors (Gałka et al., 2023; Oswald et al., 2003; Sim et al., 2019, 2021). With this in mind, our cores were all collected at spots free of hydrological and topographic variations, aiming to minimize potential local influences and maximize their climate sensitivities.

4.3. Carbon Accumulation Responses to Ecosystem and Climate Changes

The high aCAR of *Sphagnum* peat at UIC indicates the ongoing vigorous growth of peat patches with a stable input of plant litter, which, as predicted from the conceptual model for FBT (Loisel & Bunsen, 2020; Loisel & Yu, 2013), may have profound consequences for their C sink capacities (Figure 6b; Table 2). Recent studies reveal that, in addition to their known low decomposability of recalcitrant litter and inhibited microbial decomposition in acidic environments (Clymo & Hayward, 1982; Rydin & Jeglum, 2013), *Sphagnum* mosses have unique biochemical features to promote mineral protection of OM (Zhao et al., 2023). This mechanism is more important when peat layers are still thin just above mineral soils as in our cases where new colonization of *Sphagnum* mosses in peat patches would stabilize the historical C pool and self-protect new *Sphagnum* peat accumulation. However, we cannot quantify the changes in C balance from sedge peat to *Sphagnum* peat from aCAR data alone because young peat has only undergone a shorter time of decomposition (Young et al., 2019, 2021; Zhang & Väliranta, 2024). To address this "aCAR" problem, new approaches and expanded data sets are needed to construct true C accumulation rates or net C balance by accounting for their differential decomposition histories (Loisel & Yu, 2013; Young et al., 2021; Zhang et al., 2020). However, the same timing of *Sphagnum* onsets described earlier and the same pattern of recent aCAR between UIC and other Alaskan peatlands including KRP (Loisel & Yu, 2013; Taylor et al., 2019) perhaps at least imply that tundra peat patches are similar to permafrost peatlands in terms of both ecosystem processes and C dynamics (Figure 7). We, therefore, infer from these high similarities that these meter-scale, shallow peat patches have already developed the network of stabilizing feedbacks between hydrological and ecological processes that characterize mature peatlands to maintain their resilience and stability on the landscape (Belyea & Baird, 2006; Morris et al., 2011).

Although the above "aCAR problem" remains to be addressed, we find from the well-dated core UIC13-3 that after *Sphagnum* peat was established, a period of decreased aCAR within the increasing aCAR trend coincides in timing with the aforementioned cooling reversal of 1950–1975 CE documented by instrumental and multi-proxy data (Figure 4b). These distinguishable responses of C accumulation to subtle temperature changes at decadal timescales provide tentative support for the idea that climate warming may enhance the C sink capacity of peat-forming ecosystems in high-latitude regions by strongly increasing the rate of plant production while climate cooling may result in the opposite (Charman et al., 2013; Gallego-Sala et al., 2018; Yu et al., 2009). As we have already seen the evidence that these peat patches function like peatlands, if peat patches further grow with warming and enhance their C sink capacity in the coming decades or centuries, these peat patches may eventually coalesce to form an "Arctic peatland."

4.4. Carbon-Cycle Implications and Future Priorities

The current C balance of Arctic tundra is uncertain, with contrasting signs reported in literature (Commane et al., 2017; Euskirchen et al., 2017; McGuire et al., 2012; Ramage et al., 2024; Virkkala et al., 2021). For the Toolik Lake area, tundra ecosystems are sources of CO_2 due to strong emissions during non-growing seasons (Commane et al., 2017; Euskirchen et al., 2017), and the C loss is thought to accelerate in the future primarily owing to the positive feedback from permafrost thaw that further increases ecosystem respiration (Hugelius et al., 2020; Schuur et al., 2009; Turetsky et al., 2020). In this study, we document the young formation ages, dynamic changes, and ongoing vigorous growth of shallow, patchy peat deposits on Alaskan tussock tundra and demonstrate the underappreciated, potential role of these northernmost peat-forming frontiers in strongly shifting the future trajectory of the pan-Arctic C cycle as the initial stage of new peatland formation. Indeed, C flux measurements at the Toolik Lake area have shown that tussock tundra, where ~13% of the surface has developed peat patches at UIC based on our field survey, is the weakest C source (~30 $gC/m^2/yr$) compared to heath and wet sedge tundra (Euskirchen et al., 2017). Additionally, our observations suggest that the occurrence of new peat in Arctic tundra can occur on gentle hillslopes widespread on continents and did not rely on peculiar topography and local waterlogging conditions that typically characterize peat-forming wetlands (Kleinen et al., 2012). Therefore, the potential future peatland-rich landscape in the Arctic as hotspots of C sequestration may provide negative

feedback to counter C losses in response to warming. This process can be thought of as an analog for the explosive expansion of modern boreal and sub-Arctic peatlands that occurred during the early Holocene (Jones & Yu, 2010; MacDonald et al., 2006; Yu et al., 2010), when atmospheric CO_2 concentration declined slowly due to the increased land biosphere C uptake (Yu et al., 2011).

Below, we outline several important implications of this study with recommended future priorities, which will enhance the research agenda for understanding whether and how peatlands migrate poleward in a future warming climate.

First, the areal distribution, C storage, and C sequestration potential of similar tundra peat patches are likely severely underestimated in other parts of the world (Juselius et al., 2022). From our helicopter expedition and ground truthing, we have found that such peat patches are widespread on NSA and more developed in other Alaskan areas that have not yet been investigated, compared to our main study site of UIC (Figures 2a and 2f). Metcalfe et al. (2018) pointed out that our understanding of climate change impacts across the Arctic is heavily biased toward studies conducted at the Toolik Lake area, with outstanding gaps in the Canadian Arctic Archipelago and the Arctic coastline of Russia. Therefore, future studies should aim to collect more new data from pan-Arctic tundra peat patches in a larger spatial scale and in combination with data synthesis and permafrost peatland/wetland records to document the continental-scale patterns of tundra soil and peat C dynamics.

Second, based on our paleoecological records, we have specifically hypothesized that the initial peat buildup on tundra soils may benefit from cooling-driven OM preservation and microclimate feedback and that the onset of *Sphagnum* growth may further shift the balance between OM production and decomposition or enhance mineral-associated OM protection. To firmly test these hypotheses, we need incubation experiments, in situ microclimate observations, and biochemical composition measurements to improve our knowledge about the relevant mechanisms that control tundra peat formation and persistence (Du et al., 2022; Knoblauch et al., 2018; Treat et al., 2014; von Oppen et al., 2022; Zhao et al., 2023).

Finally, this study also underscores the urgent need to incorporate and improve ecosystem processes related to peat formation and accumulation into Earth system models to accurately predict the future trajectory of C balance over Arctic tundra or northern peatlands (Loisel et al., 2021). Although several recent studies have made important progress toward this goal (Chaudhary et al., 2020; Müller & Joos, 2021; Qiu et al., 2020; Stocker et al., 2014; Zhao & Zhuang, 2023), not all model predictions incorporate interactions between peatlands and non-peatlands, dynamic vegetation changes, and peatland area changes, which we find to be important in simulating the possible transformation from tundra soils to mature peatlands. For example, future predictions using a peatland-specific dynamic global vegetation model (Chaudhary et al., 2022) or a statistical climate-space model (Gallego-Sala et al., 2018) did not have peatland C accumulation on NSA because it is not within the current peatland area. Another study using a peatland-specific land surface model can simulate a small increase in peatland area and C stock on NSA but did not consider vegetation changes (Qiu et al., 2020), despite the statistical climate-space model predicting that it is a region suitable for *Sphagnum* moss expansion (Ma et al., 2022), as already found in our paleoecological records. Therefore, it is difficult to scale up our data at the current stage due to the limitation of these model simulations.

5. Conclusion

We use multi-core and multi-proxy paleo-records from the NSA to reveal the genesis and evolution of peat patches on the Arctic tundra landscape, which fill the fundamental knowledge gap about the connections in ecosystem functions and processes between shallow peat patches and mature peatlands in northern high latitudes. We find that peat patches initiated during the LIA as sedge peat above mineral soils and shifted to *Sphagnum* peat during the recent warming period with high carbon accumulation rates. This result does not fully support our aforementioned first hypothesis that peat patches initiated during warm periods, leading us to propose that organic matter preservation by climate cooling is an overlooked mechanism for initial peat buildup. It does, however, fully support our second hypothesis that the development sequence and carbon sink capacity of peat patches are climate-driven for our sites that are not associated with any local permafrost-related terrain dynamics. By comparing with counterpart records of permafrost peatlands in the same region, we find that tundra peat patches and permafrost peatlands show the same timing and pattern of recent shifts in dominant vegetation and carbon accumulation toward a potentially stronger carbon sink since the recent warming period. This result supports our third hypothesis and indicates that shallow peat patches may have already developed the same ecohydrological

feedback system as mature peatlands to maintain their long-term stability on the landscape. Taken together, our study supports the UNEP's report that underscores from a climate policy point of view the global importance of widespread shallow peat (UNEP, 2022), which is understudied and potentially will transform our understanding of diverse peat-forming ecosystems and their role in the global carbon cycle if new observational data, laboratory experiments, model simulations become available.

Data Availability Statement

All data generated in this study are available on Figshare at: https://doi.org/10.6084/m9.figshare.25728360.v1 (Cleary, 2024). Radiocarbon data are available in Table S1 in Supporting Information S1. The Arctic 2k temperature reconstruction can be accessed from McKay and Kaufman (2014). The Utqiagvik (Barrow) temperature data can be accessed at: https://www.ncei.noaa.gov/cdo-web/datasets (NOAA/NCEI, 2024). Modern plant C/N, δ^{13}C, and δ^{15}N data can be accessed at: https://doi.org/10.6073/pasta/329191b51f7c934d72974eaf0f9bcff9 (Shaver & Yano, 2016). Peat core database used to generate Figure 1 is from Hugelius et al. (2020). The tundra area is defined based on the ERA5 reanalysis product (Hersbach et al., 2020). Age-depth models are developed using the "clam" package on the R program (Blaauw, 2010). The macrofossil and pollen diagrams are made on the Tilia program, available from https://www.neotomadb.org/apps/tilia (Grimm, 1987).

References

Barber, K. E., Chambers, F. M., & Maddy, D. (2003). Holocene palaeoclimates from peat stratigraphy: Macrofossil proxy climate records from three oceanic raised bogs in England and Ireland. *Quaternary Science Reviews*, *22*(5), 521–539. https://doi.org/10.1016/S0277-3791(02)00185-3

Beilman, D. W., Vitt, D. H., & Halsey, L. A. (2001). Localized permafrost peatlands in western Canada: Definition, distributions, and degradation. *Arctic Antarctic and Alpine Research*, *33*(1), 70–77. https://doi.org/10.1080/15230430.2001.12003406

Belyea, L. R. (2009). Nonlinear dynamics of peatlands and potential feedbacks on the climate system. In A. J. Baird, L. R. Belyea, X. Comas, A. S. Reeve, & L. D. Slater (Eds.), *Carbon cycling in northern Peatlands* (pp. 5–18). American Geophysical Union.

Belyea, L. R., & Baird, A. J. (2006). Beyond "The limits to peat bog growth": Cross-scale feedback in peatland development. *Ecological Monographs*, *76*(3), 299–322. https://doi.org/10.1890/0012-9615(2006)076[0299:BTLTPB]2.0.CO;2

Blaauw, M. (2010). Methods and code for 'classical' age-modelling of radiocarbon sequences. *Quaternary Geochronology*, *5*(5), 512–518. https://doi.org/10.1016/j.quageo.2010.01.002

Bockheim, J. G., Everett, L. R., Hinkel, K. M., Nelson, F. E., & Brown, J. (1999). Soil organic carbon storage and distribution in Arctic tundra, Barrow, Alaska. *Soil Science Society of America Journal*, *63*(4), 934–940. https://doi.org/10.2136/sssaj1999.634934x

Bouskill, N. J., Riley, W. J., Zhu, Q., Mekonnen, Z. A., & Grant, R. F. (2020). Alaskan carbon-climate feedbacks will be weaker than inferred from short-term experiments. *Nature Communications*, *11*(1), 5798. https://doi.org/10.1038/s41467-020-19574-3

Bradford, M. A., Wieder, W. R., Bonan, G. B., Fierer, N., Raymond, P. A., & Crowther, T. W. (2016). Managing uncertainty in soil carbon feedbacks to climate change. *Nature Climate Change*, *6*(8), 751–758. https://doi.org/10.1038/nclimate3071

Broder, T., Blodau, C., Biester, H., & Knorr, K. H. (2012). Peat decomposition records in three pristine ombrotrophic bogs in southern Patagonia. *Biogeosciences*, *9*(4), 1479–1491. https://doi.org/10.5194/bg-9-1479-2012

Calkin, P. E. (1988). Holocene glaciation of Alaska (and adjoining Yukon Territory, Canada). *Quaternary Science Reviews*, *7*(2), 159–184. https://doi.org/10.1016/0277-3791(88)90004-2

Charman, D. J., Beilman, D. W., Blaauw, M., Booth, R. K., Brewer, S., Chambers, F. M., et al. (2013). Climate-related changes in peatland carbon accumulation during the last millennium. *Biogeosciences*, *10*(2), 929–944. https://doi.org/10.5194/bg-10-929-2013

Chaudhary, N., Westermann, S., Lamba, S., Shurpali, N., Sannel, A. B. K., Schurgers, G., et al. (2020). Modelling past and future peatland carbon dynamics across the pan-Arctic. *Global Change Biology*, *26*(7), 4119–4133. https://doi.org/10.1111/gcb.15099

Chaudhary, N., Zhang, W., Lamba, S., & Westermann, S. (2022). Modeling pan-Arctic peatland carbon dynamics under alternative warming scenarios. *Geophysical Research Letters*, *49*(10), e2021GL095276. https://doi.org/10.1029/2021GL095276

Cleary, K. (2024). Tundra peat patches core data [Dataset]. *Figshare*. https://doi.org/10.6084/m9.figshare.25728360.v1

Cleary, K. G. (2015). *Shrub expansion, Sphagnum peat growth, and carbon sequestration in Arctic tundra on the North Slope of Alaska* (MS Thesis). Lehigh University.

Clymo, R. S. (1984). The limits to peat bog growth. *Philosophical Transactions of the Royal Society of London B Biological Sciences*, *303*(1117), 605–654. https://doi.org/10.1098/rstb.1984.0002

Clymo, R. S., & Hayward, P. M. (1982). The ecology of *Sphagnum*. In A. J. E. Smith (Ed.), *Bryophyte ecology* (pp. 229–289). Springer.

Commane, R., Lindaas, J., Benmergui, J., Luus, K. A., Chang, R. Y.-W., Daube, B. C., et al. (2017). Carbon dioxide sources from Alaska driven by increasing early winter respiration from Arctic tundra. *Proceedings of the National Academy of Sciences*, *114*(21), 5361–5366. https://doi.org/10.1073/pnas.1618567114

Daley, T. J., Barber, K. E., Street-Perrott, F. A., Loader, N. J., Marshall, J. D., Crowley, S. F., & Fisher, E. H. (2010). Holocene climate variability revealed by oxygen isotope analysis of *Sphagnum* cellulose from Walton Moss, northern England. *Quaternary Science Reviews*, *29*(13), 1590–1601. https://doi.org/10.1016/j.quascirev.2009.09.017

Daniels, W. C., Russell, J. M., Giblin, A. E., Welker, J. M., Klein, E. S., & Huang, Y. (2017). Hydrogen isotope fractionation in leaf waxes in the Alaskan Arctic tundra. *Geochimica et Cosmochimica Acta*, *213*, 216–236. https://doi.org/10.1016/j.gca.2017.06.028

Dansgaard, W. (1964). Stable isotopes in precipitation. *Tellus*, *16*(4), 436–468. https://doi.org/10.3402/tellusa.v16i4.8993

de Klerk, P., Donner, N., Joosten, H., Karpov, N. S., Minke, M., Seifert, N., & Theuerkauf, M. (2009). Vegetation patterns, recent pollen deposition and distribution of non-pollen palynomorphs in a polygon mire near Chokurdakh (NE Yakutia, NE Siberia). *Boreas*, *38*(1), 39–58. https://doi.org/10.1111/j.1502-3885.2008.00036.x

de Vrese, P., & Brovkin, V. (2021). Timescales of the permafrost carbon cycle and legacy effects of temperature overshoot scenarios. *Nature Communications*, *12*(1), 2688. https://doi.org/10.1038/s41467-021-23010-5

Du, R., Peng, X., Frauenfeld, O. W., Sun, W., Liang, B., Chen, C., et al. (2022). The role of peat on permafrost thaw based on field observations. *Catena*, *208*, 105772. https://doi.org/10.1016/j.catena.2021.105772

Eisner, W. R. (1991). Palynological analysis of a peat core from Imnavait Creek, the North Slope, Alaska. *Arctic*, *44*(4), 279–282. https://doi.org/10.14430/arctic1551

Euskirchen, E. S., Bret-Harte, M. S., Shaver, G. R., Edgar, C. W., & Romanovsky, V. E. (2017). Long-term release of carbon dioxide from Arctic tundra ecosystems in Alaska. *Ecosystems*, *20*(5), 960–974. https://doi.org/10.1007/s10021-016-0085-9

Fewster, R. E., Morris, P. J., Ivanovic, R. F., Swindles, G. T., Peregon, A. M., & Smith, C. J. (2022). Imminent loss of climate space for permafrost peatlands in Europe and Western Siberia. *Nature Climate Change*, *12*(4), 373–379. https://doi.org/10.1038/s41558-022-01296-7

Fu, Y., Li, Y., & Yu, Z. (2022). Last millennium hydroclimate and atmospheric circulation change in Northeast China: A dual δ^{13}C and δ^{18}O approach from a mountaintop *Sphagnum* bog. *Quaternary Science Reviews*, *295*, 107781. https://doi.org/10.1016/j.quascirev.2022.107781

Gaglioti, B. V., Mann, D. H., Wooller, M. J., Jones, B. M., Wiles, G. C., Groves, P., et al. (2017). Younger-Dryas cooling and sea-ice feedbacks were prominent features of the Pleistocene-Holocene transition in Arctic Alaska. *Quaternary Science Reviews*, *169*, 330–343. https://doi.org/10.1016/j.quascirev.2017.05.012

Gałka, M., Diaconu, A.-C., Cwanek, A., Hedenäs, L., Knorr, K.-H., Kołaczek, P., et al. (2023). Climate-induced hydrological fluctuations shape Arctic Alaskan peatland plant communities. *Science of the Total Environment*, *905*, 167381. https://doi.org/10.1016/j.scitotenv.2023.167381

Gałka, M., Swindles, G. T., Szal, M., Fulweber, R., & Feurdean, A. (2018). Response of plant communities to climate change during the late Holocene: Palaeoecological insights from peatlands in the Alaskan Arctic. *Ecological Indicators*, *85*, 525–536. https://doi.org/10.1016/j.ecolind.2017.10.062

Gallego-Sala, A. V., Charman, D. J., Brewer, S., Page, S. E., Prentice, I. C., Friedlingstein, P., et al. (2018). Latitudinal limits to the predicted increase of the peatland carbon sink with warming. *Nature Climate Change*, *8*(10), 907–913. https://doi.org/10.1038/s41558-018-0271-1

Goryachkin, S. V., Karavaeva, N. A., Targulian, V. O., & Glazov, M. V. (1999). Arctic soils: Spatial distribution, zonality and transformation due to global change. *Permafrost and Periglacial Processes*, *10*(3), 235–250. https://doi.org/10.1002/(SICI)1099-1530(199907/09)10:3<235::AID-PPP320>3.0.CO;2-4

Granlund, L., Vesakoski, V., Sallinen, A., Kolari, T. H. M., Wolff, F., & Tahvanainen, T. (2022). Recent lateral expansion of *Sphagnum* bogs over central fen areas of boreal aapa mire complexes. *Ecosystems*, *25*(7), 1455–1475. https://doi.org/10.1007/s10021-021-00726-5

Grimm, E. C. (1987). CONISS: A FORTRAN 77 program for stratigraphically constrained cluster analysis by the method of incremental sum of squares. *Computers & Geosciences*, *13*(1), 13–35. https://doi.org/10.1016/0098-3004(87)90022-7

Hamilton, T. D. (1986). Late Cenozoic glaciation of the central Brooks range. In T. D. Hamilton, K. M. Reed, & R. M. Thorson (Eds.), *Glaciation in Alaska: The geologic record* (pp. 9–49). Alaska Geological Society.

Harden, J. W., Mark, R. K., Sundquist, E. T., & Stallard, R. F. (1992). Dynamics of soil carbon during deglaciation of the Laurentide ice sheet. *Science*, *258*(5090), 1921–1924. https://doi.org/10.1126/science.258.5090.1921

Hersbach, H., Bell, B., Berrisford, P., Hirahara, S., Horányi, A., Muñoz-Sabater, J., et al. (2020). The ERA5 global reanalysis. *Quarterly Journal of the Royal Meteorological Society*, *146*(730), 1999–2049. https://doi.org/10.1002/qj.3803

Hu, F. S., Higuera, P. E., Duffy, P., Chipman, M. L., Rocha, A. V., Young, A. M., et al. (2015). Arctic tundra fires: Natural variability and responses to climate change. *Frontiers in Ecology and the Environment*, *13*(7), 369–377. https://doi.org/10.1890/150063

Hu, F. S., Ito, E., Brown, T. A., Curry, B. B., & Engstrom, D. R. (2001). Pronounced climatic variations in Alaska during the last two millennia. *Proceedings of the National Academy of Sciences*, *98*(19), 10552–10556. https://doi.org/10.1073/pnas.181333798

Hua, Q., Turnbull, J. C., Santos, G. M., Rakowski, A. Z., Ancapichún, S., De Pol-Holz, R., et al. (2022). Atmospheric radiocarbon for the period 1950–2019. *Radiocarbon*, *64*(4), 723–745. https://doi.org/10.1017/RDC.2021.95

Hugelius, G., Loisel, J., Chadburn, S., Jackson, R. B., Jones, M., MacDonald, G., et al. (2020). Large stocks of peatland carbon and nitrogen are vulnerable to permafrost thaw. *Proceedings of the National Academy of Sciences*, *117*(34), 20438–20446. https://doi.org/10.1073/pnas.1916387117

Hugelius, G., Strauss, J., Zubrzycki, S., Harden, J. W., Schuur, E. A. G., Ping, C. L., et al. (2014). Estimated stocks of circumpolar permafrost carbon with quantified uncertainty ranges and identified data gaps. *Biogeosciences*, *11*(23), 6573–6593. https://doi.org/10.5194/bg-11-6573-2014

Hughes, P. D. M., & Barber, K. E. (2003). Mire development across the fen–bog transition on the Teifi floodplain at Tregaron Bog, Ceredigion, Wales, and a comparison with 13 other raised bogs. *Journal of Ecology*, *91*(2), 253–264. https://doi.org/10.1046/j.1365-2745.2003.00762.x

Huryn, A., & Hobbie, J. (2012). *Land of extremes: A natural history of the Arctic North Slope of Alaska*. University of Alaska Press.

IPCC. (2007). Climate Change 2007: Working Group I: The physical science basis.

Jia, G. J., Epstein, H. E., & Walker, D. A. (2003). Greening of arctic Alaska, 1981–2001. *Geophysical Research Letters*, *30*(20), 2067. https://doi.org/10.1029/2003GL018268

Jones, M. C., Peteet, D. M., & Sambrotto, R. (2010). Late-glacial and Holocene δ^{15}N and δ^{13}C variation from a Kenai Peninsula, Alaska peatland. *Palaeogeography, Palaeoclimatology, Palaeoecology*, *293*(1), 132–143. https://doi.org/10.1016/j.palaeo.2010.05.007

Jones, M. C., & Yu, Z. (2010). Rapid deglacial and early Holocene expansion of peatlands in Alaska. *Proceedings of the National Academy of Sciences*, *107*(16), 7347–7352. https://doi.org/10.1073/pnas.0911387107

Joosten, H., & Clarke, D. (2002). *Wise use of mires and Peatlands: Background and principles including a framework for decision-making*. International Mire Conservation Group and International Peatland Society.

Juselius, T., Ravolainen, V., Zhang, H., Piilo, S., Müller, M., Gallego-Sala, A., & Väliranta, M. (2022). Newly initiated carbon stock, organic soil accumulation patterns and main driving factors in the High Arctic Svalbard, Norway. *Scientific Reports*, *12*(1), 4679. https://doi.org/10.1038/s41598-022-08652-9

Kaislahti Tillman, P., Holzkämper, S., Andersen, T. J., Hugelius, G., Kuhry, P., & Oksanen, P. (2013). Stable isotopes in *Sphagnum fuscum* peat as late-Holocene climate proxies in northeastern European Russia. *The Holocene*, *23*(10), 1381–1390. https://doi.org/10.1177/0959683613489580

Kaufman, D. S., Schneider, D. P., McKay, N. P., Ammann, C. M., Bradley, R. S., Briffa, K. R., et al. (2009). Recent warming reverses long-term Arctic cooling. *Science*, *325*(5945), 1236–1239. https://doi.org/10.1126/science.1173983

Kim, J., Kim, Y., Zona, D., Oechel, W., Park, S.-J., Lee, B.-Y., et al. (2021). Carbon response of tundra ecosystems to advancing greenup and snowmelt in Alaska. *Nature Communications*, *12*(1), 6879. https://doi.org/10.1038/s41467-021-26876-7

Klaminder, J., Yoo, K., & Giesler, R. (2009). Soil carbon accumulation in the dry tundra: Important role played by precipitation. *Journal of Geophysical Research*, *114*(G4), G04005. https://doi.org/10.1029/2009JG000947

Klein, E. S., Yu, Z., & Booth, R. K. (2013). Recent increase in peatland carbon accumulation in a thermokarst lake basin in southwestern Alaska. *Palaeogeography, Palaeoclimatology, Palaeoecology*, *392*, 186–195. https://doi.org/10.1016/j.palaeo.2013.09.009

Kleinen, T., Brovkin, V., & Schuldt, R. J. (2012). A dynamic model of wetland extent and peat accumulation: Results for the Holocene. *Biogeosciences*, *9*(1), 235–248. https://doi.org/10.5194/bg-9-235-2012

Knoblauch, C., Beer, C., Liebner, S., Grigoriev, M. N., & Pfeiffer, E.-M. (2018). Methane production as key to the greenhouse gas budget of thawing permafrost. *Nature Climate Change*, *8*(4), 309–312. https://doi.org/10.1038/s41558-018-0095-z

Kuptsova, V., & Chakov, V. (2022). Species composition of the bryophytes in mires of Big Shantar Island (National Park «Shantarskie ostrova»). Paper presented at the IOP Conference Series: Earth and Environmental Science, VI International Field Symposium West Siberian Peatlands and Carbon Cycle: Past and Present, Khanty-Mansiysk, Russia.

Leuenberger, M. (2007). To what extent can ice core data contribute to the understanding of plant ecological developments of the past? In T. E. Dawson & R. T. W. Siegwolf (Eds.), *Stable isotopes as indicators of ecological change* (Vol. 1, pp. 211–233). Elsevier. https://doi.org/10.1016/s1936-7961(07)01014-7

Loader, N. J., Robertson, I., Barker, A. C., Switsur, V. R., & Waterhouse, J. S. (1997). An improved technique for the batch processing of small wholewood samples to α-cellulose. *Chemical Geology*, *136*(3), 313–317. https://doi.org/10.1016/S0009-2541(96)00133-7

Loisel, J., & Bunsen, M. (2020). Abrupt fen-bog transition across southern Patagonia: Timing, causes, and impacts on carbon sequestration. *Frontiers in Ecology and Evolution*, *8*. https://doi.org/10.3389/fevo.2020.00273

Loisel, J., Gallego-Sala, A. V., Amesbury, M. J., Magnan, G., Anshari, G., Beilman, D. W., et al. (2021). Expert assessment of future vulnerability of the global peatland carbon sink. *Nature Climate Change*, *11*(1), 70–77. https://doi.org/10.1038/s41558-020-00944-0

Loisel, J., Gallego-Sala, A. V., & Yu, Z. (2012). Global-scale pattern of peatland *Sphagnum* growth driven by photosynthetically active radiation and growing season length. *Biogeosciences*, *9*(7), 2737–2746. https://doi.org/10.5194/bg-9-2737-2012

Loisel, J., & Yu, Z. (2013). Recent acceleration of carbon accumulation in a boreal peatland, south central Alaska. *Journal of Geophysical Research: Biogeosciences*, *118*(1), 41–53. https://doi.org/10.1029/2012JG001978

Loso, M. G. (2009). Summer temperatures during the Medieval Warm Period and Little Ice Age inferred from varved proglacial lake sediments in southern Alaska. *Journal of Paleolimnology*, *41*(1), 117–128. https://doi.org/10.1007/s10933-008-9264-9

Luo, Y. (2007). Terrestrial carbon–cycle feedback to climate warming. *Annual Review of Ecology Evolution and Systematics*, *38*(1), 683–712. https://doi.org/10.1146/annurev.ecolsys.38.091206.095808

Ma, X.-Y., Xu, H., Cao, Z.-Y., Shu, L., & Zhu, R.-L. (2022). Will climate change cause the global peatland to expand or contract? Evidence from the habitat shift pattern of *Sphagnum* mosses. *Global Change Biology*, *28*(21), 6419–6432. https://doi.org/10.1111/gcb.16354

MacDonald, G. M., Beilman, D. W., Kremenetski, K. V., Sheng, Y., Smith, L. C., & Velichko, A. A. (2006). Rapid early development of circumarctic peatlands and atmospheric CH_4 and CO_2 variations. *Science*, *314*(5797), 285–288. https://doi.org/10.1126/science.1131722

Mack, M. C., Bret-Harte, M. S., Hollingsworth, T. N., Jandt, R. R., Schuur, E. A. G., Shaver, G. R., & Verbyla, D. L. (2011). Carbon loss from an unprecedented Arctic tundra wildfire. *Nature*, *475*(7357), 489–492. https://doi.org/10.1038/nature10283

Magnan, G., Sanderson, N. K., Piilo, S., Pratte, S., Väliranta, M., van Bellen, S., et al. (2022). Widespread recent ecosystem state shifts in high-latitude peatlands of northeastern Canada and implications for carbon sequestration. *Global Change Biology*, *28*(5), 1919–1934. https://doi.org/10.1111/gcb.16032

McCrystall, M. R., Stroeve, J., Serreze, M., Forbes, B. C., & Screen, J. A. (2021). New climate models reveal faster and larger increases in Arctic precipitation than previously projected. *Nature Communications*, *12*(1), 6765. https://doi.org/10.1038/s41467-021-27031-y

McGuire, A. D., Christensen, T. R., Hayes, D., Heroult, A., Euskirchen, E., Kimball, J. S., et al. (2012). An assessment of the carbon balance of Arctic tundra: Comparisons among observations, process models, and atmospheric inversions. *Biogeosciences*, *9*(8), 3185–3204. https://doi.org/10.5194/bg-9-3185-2012

McKay, N. P., & Kaufman, D. S. (2014). An extended Arctic proxy temperature database for the past 2,000 years. *Scientific Data*, *1*(1), 140026. https://doi.org/10.1038/sdata.2014.26

Metcalfe, D. B., Hermans, T. D. G., Ahlstrand, J., Becker, M., Berggren, M., Björk, R. G., et al. (2018). Patchy field sampling biases understanding of climate change impacts across the Arctic. *Nature Ecology & Evolution*, *2*(9), 1443–1448. https://doi.org/10.1038/s41559-018-0612-5

Morris, P. J., Belyea, L. R., & Baird, A. J. (2011). Ecohydrological feedbacks in peatland development: A theoretical modelling study. *Journal of Ecology*, *99*(5), 1190–1201. https://doi.org/10.1111/j.1365-2745.2011.01842.x

Morris, P. J., Swindles, G. T., Valdes, P. J., Ivanovic, R. F., Gregoire, L. J., Smith, M. W., et al. (2018). Global peatland initiation driven by regionally asynchronous warming. *Proceedings of the National Academy of Sciences*, *115*(19), 4851–4856. https://doi.org/10.1073/pnas.1717838115

Moskal, T. D., Leskiw, L., Naeth, M. A., & Chanasyk, D. S. (2001). Effect of organic carbon (peat) on moisture retention of peat:mineral mixes. *Canadian Journal of Soil Science*, *81*(2), 205–211. https://doi.org/10.4141/S00-011

Müller, J., & Joos, F. (2021). Committed and projected future changes in global peatlands – Continued transient model simulations since the Last Glacial Maximum. *Biogeosciences*, *18*(12), 3657–3687. https://doi.org/10.5194/bg-18-3657-2021

Myers-Smith, I. H., Forbes, B. C., Wilmking, M., Hallinger, M., Lantz, T., Blok, D., et al. (2011). Shrub expansion in tundra ecosystems: Dynamics, impacts and research priorities. *Environmental Research Letters*, *6*(4), 045509. https://doi.org/10.1088/1748-9326/6/4/045509

Myers-Smith, I. H., Kerby, J. T., Phoenix, G. K., Bjerke, J. W., Epstein, H. E., Assmann, J. J., et al. (2020). Complexity revealed in the greening of the Arctic. *Nature Climate Change*, *10*(2), 106–117. https://doi.org/10.1038/s41558-019-0688-1

Natali, S. M., Watts, J. D., Rogers, B. M., Potter, S., Ludwig, S. M., Selbmann, A.-K., et al. (2019). Large loss of CO_2 in winter observed across the northern permafrost region. *Nature Climate Change*, *9*(11), 852–857. https://doi.org/10.1038/s41558-019-0592-8

Nichols, J. E., Peteet, D. M., Frolking, S., & Karavias, J. (2017). A probabilistic method of assessing carbon accumulation rate at Imnavait Creek Peatland, Arctic long term ecological research station, Alaska. *Journal of Quaternary Science*, *32*(5), 579–586. https://doi.org/10.1002/jqs.2952

NOAA/NCEI. (2024). Global summary of the month [Dataset]. *NOAA/NCEI Climate Data Online*. https://www.ncei.noaa.gov/cdo-web/datasets

Oswald, W. W., Brubaker, L. B., Hu, F. S., & Kling, G. W. (2003). Holocene pollen records from the central Arctic Foothills, northern Alaska: Testing the role of substrate in the response of tundra to climate change. *Journal of Ecology*, *91*(6), 1034–1048. https://doi.org/10.1046/j.1365-2745.2003.00833.x

Payne, R. J., Malysheva, E., Tsyganov, A., Pampura, T., Novenko, E., Volkova, E., et al. (2016). A multi-proxy record of Holocene environmental change, peatland development and carbon accumulation from Staroselsky Moch peatland, Russia. *The Holocene*, *26*(2), 314–326. https://doi.org/10.1177/0959683615608692

Piilo, S. R., Korhola, A., Heiskanen, L., Tuovinen, J.-P., Aurela, M., Juutinen, S., et al. (2020). Spatially varying peatland initiation, Holocene development, carbon accumulation patterns and radiative forcing within a subarctic fen. *Quaternary Science Reviews*, *248*, 106596. https://doi.org/10.1016/j.quascirev.2020.106596

Piilo, S. R., Väliranta, M. M., Amesbury, M. J., Aquino-López, M. A., Charman, D. J., Gallego-Sala, A., et al. (2023). Consistent centennial-scale change in European sub-Arctic peatland vegetation toward *Sphagnum* dominance—Implications for carbon sink capacity. *Global Change Biology*, *29*(6), 1530–1544. https://doi.org/10.1111/gcb.16554

Ping, C.-L., Michaelson, G. J., Jorgenson, M. T., Kimble, J. M., Epstein, H., Romanovsky, V. E., & Walker, D. A. (2008). High stocks of soil organic carbon in the North American Arctic region. *Nature Geoscience*, *1*(9), 615–619. https://doi.org/10.1038/ngeo284

Qian, H., Joseph, R., & Zeng, N. (2010). Enhanced terrestrial carbon uptake in the northern high latitudes in the 21st century from the coupled carbon cycle climate model intercomparison project model projections. *Global Change Biology*, *16*(2), 641–656. https://doi.org/10.1111/j.1365-2486.2009.01989.x

Qiu, C., Zhu, D., Ciais, P., Guenet, B., & Peng, S. (2020). The role of northern peatlands in the global carbon cycle for the 21st century. *Global Ecology and Biogeography*, *29*(5), 956–973. https://doi.org/10.1111/geb.13081

Quik, C., Palstra, S. W. L., van Beek, R., van der Velde, Y., Candel, J. H. J., van der Linden, M., et al. (2022). Dating basal peat: The geochronology of peat initiation revisited. *Quaternary Geochronology*, *72*, 101278. https://doi.org/10.1016/j.quageo.2022.101278

Ramage, J., Kuhn, M., Virkkala, A.-M., Voigt, C., Marushchak, M. E., Bastos, A., et al. (2024). The net GHG balance and budget of the permafrost region (2000–2020) from ecosystem flux upscaling. *Global Biogeochemical Cycles*, *38*(4), e2023GB007953. https://doi.org/10.1029/2023GB007953

Rantanen, M., Karpechko, A. Y., Lipponen, A., Nordling, K., Hyvärinen, O., Ruosteenoja, K., et al. (2022). The Arctic has warmed nearly four times faster than the globe since 1979. *Communications Earth & Environment*, *3*(1), 168. https://doi.org/10.1038/s43247-022-00498-3

Reimer, P. J., Austin, W. E. N., Bard, E., Bayliss, A., Blackwell, P. G., Bronk Ramsey, C., et al. (2020). The IntCal20 Northern Hemisphere radiocarbon age calibration curve (0–55 cal kBP). *Radiocarbon*, *62*(4), 725–757. https://doi.org/10.1017/RDC.2020.41

Runkle, B. R. K., Wille, C., Gažovič, M., Wilmking, M., & Kutzbach, L. (2014). The surface energy balance and its drivers in a boreal peatland fen of northwestern Russia. *Journal of Hydrology*, *511*, 359–373. https://doi.org/10.1016/j.jhydrol.2014.01.056

Rydin, H., & Jeglum, J. K. (2013). *The biology of Peatlands* (2nd ed.). Oxford University Press.

Scholten, R. C., Coumou, D., Luo, F., & Veraverbeke, S. (2022). Early snowmelt and polar jet dynamics co-influence recent extreme Siberian fire seasons. *Science*, *378*(6623), 1005–1009. https://doi.org/10.1126/science.abn4419

Schuur, E. A. G., McGuire, A. D., Schädel, C., Grosse, G., Harden, J. W., Hayes, D. J., et al. (2015). Climate change and the permafrost carbon feedback. *Nature*, *520*(7546), 171–179. https://doi.org/10.1038/nature14338

Schuur, E. A. G., Vogel, J. G., Crummer, K. G., Lee, H., Sickman, J. O., & Osterkamp, T. E. (2009). The effect of permafrost thaw on old carbon release and net carbon exchange from tundra. *Nature*, *459*(7246), 556–559. https://doi.org/10.1038/nature08031

Shaver, G., & Yano, Y. (2016). Bulk concentration and isotopic information of plant C and N in green leaves and tissues collected from Imnavait watershed during 2003-2005 ver 4 [Dataset]. *Environmental Data Initiative*. https://doi.org/10.6073/pasta/329191b51f7c934d72974eaf0f9bcff9

Sim, T. G., Swindles, G. T., Morris, P. J., Baird, A. J., Cooper, C. L., Gallego-Sala, A. V., et al. (2021). Divergent responses of permafrost peatlands to recent climate change. *Environmental Research Letters*, *16*(3), 034001. https://doi.org/10.1088/1748-9326/abe00b

Sim, T. G., Swindles, G. T., Morris, P. J., Gałka, M., Mullan, D., & Galloway, J. M. (2019). Pathways for ecological change in Canadian high Arctic wetlands under rapid twentieth century warming. *Geophysical Research Letters*, *46*(9), 4726–4737. https://doi.org/10.1029/2019GL082611

Sistla, S. A., Moore, J. C., Simpson, R. T., Gough, L., Shaver, G. R., & Schimel, J. P. (2013). Long-term warming restructures Arctic tundra without changing net soil carbon storage. *Nature*, *497*(7451), 615–618. https://doi.org/10.1038/nature12129

Stocker, B. D., Spahni, R., & Joos, F. (2014). DYPTOP: A cost-efficient TOPMODEL implementation to simulate sub-grid spatio-temporal dynamics of global wetlands and peatlands. *Geoscientific Model Development*, *7*(6), 3089–3110. https://doi.org/10.5194/gmd-7-3089-2014

Stocker, B. D., Yu, Z., Massa, C., & Joos, F. (2017). Holocene peatland and ice-core data constraints on the timing and magnitude of CO_2 emissions from past land use. *Proceedings of the National Academy of Sciences*, *114*(7), 1492–1497. https://doi.org/10.1073/pnas.1613889114

Swindles, G. T., Morris, P. J., Mullan, D., Watson, E. J., Turner, T. E., Roland, T. P., et al. (2015). The long-term fate of permafrost peatlands under rapid climate warming. *Scientific Reports*, *5*(1), 17951. https://doi.org/10.1038/srep17951

Tahvanainen, T. (2011). Abrupt ombrotrophication of a boreal aapa mire triggered by hydrological disturbance in the catchment. *Journal of Ecology*, *99*(2), 404–415. https://doi.org/10.1111/j.1365-2745.2010.01778.x

Tao, J., Zhu, Q., Riley, W. J., & Neumann, R. B. (2021). Warm-season net CO_2 uptake outweighs cold-season emissions over Alaskan North Slope tundra under current and RCP8.5 climate. *Environmental Research Letters*, *16*(5), 055012. https://doi.org/10.1088/1748-9326/abf6f5

Tape, K., Sturm, M., & Racine, C. (2006). The evidence for shrub expansion in Northern Alaska and the Pan-Arctic. *Global Change Biology*, *12*(4), 686–702. https://doi.org/10.1111/j.1365-2486.2006.01128.x

Tarnocai, C., & Stolbovoy, V. (2006). Northern Peatlands: Their characteristics, development and sensitivity to climate change. In I. P. Martini, A. Martínez Cortizas, & W. Chesworth (Eds.), *Developments in Earth surface processes* (Vol. 9, pp. 17–51). Elsevier. https://doi.org/10.1016/s0928-2025(06)09002-x

Taylor, K. E., Stouffer, R. J., & Meehl, G. A. (2012). An overview of CMIP5 and the experiment design. *Bulletin of the American Meteorological Society*, *93*(4), 485–498. https://doi.org/10.1175/BAMS-D-11-00094.1

Taylor, L. S., Swindles, G. T., Morris, P. J., Gałka, M., & Green, S. M. (2019). Evidence for ecosystem state shifts in Alaskan continuous permafrost peatlands in response to recent warming. *Quaternary Science Reviews*, *207*, 134–144. https://doi.org/10.1016/j.quascirev.2019.02.001

Todd-Brown, K. E. O., Randerson, J. T., Post, W. M., Hoffman, F. M., Tarnocai, C., Schuur, E. A. G., & Allison, S. D. (2013). Causes of variation in soil carbon simulations from CMIP5 Earth system models and comparison with observations. *Biogeosciences*, *10*(3), 1717–1736. https://doi.org/10.5194/bg-10-1717-2013

Treat, C. C., Jones, M. C., Camill, P., Gallego-Sala, A., Garneau, M., Harden, J. W., et al. (2016). Effects of permafrost aggradation on peat properties as determined from a pan-Arctic synthesis of plant macrofossils. *Journal of Geophysical Research: Biogeosciences*, *121*(1), 78–94. https://doi.org/10.1002/2015JG003061

Treat, C. C., Kleinen, T., Broothaerts, N., Dalton, A. S., Dommain, R., Douglas, T. A., et al. (2019). Widespread global peatland establishment and persistence over the last 130,000 y. *Proceedings of the National Academy of Sciences*, *116*(11), 4822–4827. https://doi.org/10.1073/pnas.1813305116

Treat, C. C., Wollheim, W. M., Varner, R. K., Grandy, A. S., Talbot, J., & Frolking, S. (2014). Temperature and peat type control CO_2 and CH_4 production in Alaskan permafrost peats. *Global Change Biology*, *20*(8), 2674–2686. https://doi.org/10.1111/gcb.12572

Turetsky, M. R., Abbott, B. W., Jones, M. C., Anthony, K. W., Olefeldt, D., Schuur, E. A. G., et al. (2020). Carbon release through abrupt permafrost thaw. *Nature Geoscience*, *13*(2), 138–143. https://doi.org/10.1038/s41561-019-0526-0

UNEP. (2022). Global Peatlands Assessment – The State of the World's Peatlands: Evidence for action toward the conservation, restoration, and sustainable management of peatlands. Main Report. Nairobi, Kenya: United Nations Environment Programme.

van Breemen, N. (1995). How *Sphagnum* bogs down other plants. *Trends in Ecology & Evolution*, *10*(7), 270–275. https://doi.org/10.1016/0169-5347(95)90007-1

Virkkala, A.-M., Aalto, J., Rogers, B. M., Tagesson, T., Treat, C. C., Natali, S. M., et al. (2021). Statistical upscaling of ecosystem CO_2 fluxes across the terrestrial tundra and boreal domain: Regional patterns and uncertainties. *Global Change Biology*, *27*(17), 4040–4059. https://doi.org/10.1111/gcb.15659

von Oppen, J., Assmann, J. J., Bjorkman, A. D., Treier, U. A., Elberling, B., Nabe-Nielsen, J., & Normand, S. (2022). Cross-scale regulation of seasonal microclimate by vegetation and snow in the Arctic tundra. *Global Change Biology*, *28*(24), 7296–7312. https://doi.org/10.1111/gcb.16426

Walker, D. A., Binnian, E., Evans, B. M., Lederer, N. D., Nordstrand, E., & Webber, P. J. (1989). Terrain, vegetation and landscape evolution of the R4D research site, Brooks Range Foothills, Alaska. *Ecography*, *12*(3), 238–261. https://doi.org/10.1111/j.1600-0587.1989.tb00844.x

Walker, D. A., Raynolds, M. K., Daniëls, F. J. A., Einarsson, E., Elvebakk, A., Gould, W. A., et al. (2005). The Circumpolar Arctic vegetation map. *Journal of Vegetation Science*, *16*(3), 267–282. https://doi.org/10.1111/j.1654-1103.2005.tb02365.x

Walker, D. A., & Walker, M. D. (1996). Terrain and vegetation of the Imnavait Creek watershed. In J. F. Reynolds & J. D. Tenhunen (Eds.), *Landscape function and disturbance in Arctic Tundra* (pp. 73–108). Springer.

Walsh, J. E. (2014). Intensified warming of the Arctic: Causes and impacts on middle latitudes. *Global and Planetary Change*, *117*, 52–63. https://doi.org/10.1016/j.gloplacha.2014.03.003

Wilkinson, S. L., Tekatch, A. M., Markle, C. E., Moore, P. A., & Waddington, J. M. (2020). Shallow peat is most vulnerable to high peat burn severity during wildfire. *Environmental Research Letters*, *15*(10), 104032. https://doi.org/10.1088/1748-9326/aba7e8

Xia, Y., Yang, Z., Sun, J., Xia, Z., & Yu, Z. (2024). Late-Holocene ecosystem dynamics and climate sensitivity of a permafrost peatland in Northeast China. *Quaternary Science Reviews*, *324*, 108466. https://doi.org/10.1016/j.quascirev.2023.108466

Xia, Z., Oppedal, L. T., Van der Putten, N., Bakke, J., & Yu, Z. (2020). Ecological response of a glacier-fed peatland to late Holocene climate and glacier changes on subantarctic South Georgia. *Quaternary Science Reviews*, *250*, 106679. https://doi.org/10.1016/j.quascirev.2020.106679

Xia, Z., Yu, Z., & Loisel, J. (2018). Centennial-scale dynamics of the southern Hemisphere Westerly Winds across the Drake passage over the past two millennia. *Geology*, *46*(10), 855–858. https://doi.org/10.1130/G40187.1

Xia, Z., Zheng, Y., Stelling, J. M., Loisel, J., Huang, Y., & Yu, Z. (2020). Environmental controls on the carbon and water (H and O) isotopes in peatland *Sphagnum* mosses. *Geochimica et Cosmochimica Acta*, *277*, 265–284. https://doi.org/10.1016/j.gca.2020.03.034

Yang, Q., Liu, Z., & Bai, E. (2023). Comparison of carbon and nitrogen accumulation rate between bog and fen phases in a pristine peatland with the fen-bog transition. *Global Change Biology*, *29*(22), 6350–6366. https://doi.org/10.1111/gcb.16915

Young, D. M., Baird, A. J., Charman, D. J., Evans, C. D., Gallego-Sala, A. V., Gill, P. J., et al. (2019). Misinterpreting carbon accumulation rates in records from near-surface peat. *Scientific Reports*, *9*(1), 17939. https://doi.org/10.1038/s41598-019-53879-8

Young, D. M., Baird, A. J., Gallego-Sala, A. V., & Loisel, J. (2021). A cautionary tale about using the apparent carbon accumulation rate (aCAR) obtained from peat cores. *Scientific Reports*, *11*(1), 9547. https://doi.org/10.1038/s41598-021-88766-8

Yu, Z., Beilman, D. W., Frolking, S., MacDonald, G. M., Roulet, N. T., Camill, P., & Charman, D. J. (2011). Peatlands and their role in the global carbon cycle. *Eos, Transactions American Geophysical Union*, *92*(12), 97–98. https://doi.org/10.1029/2011EO120001

Yu, Z., Beilman, D. W., & Jones, M. C. (2009). Sensitivity of northern peatland carbon dynamics to Holocene climate change. In A. J. Baird, L. R. Belyea, X. Comas, A. S. Reeve, & L. D. Slater (Eds.), *Carbon cycling in northern Peatlands* (pp. 55–69). American Geophysical Union.

Yu, Z., Loisel, J., Brosseau, D. P., Beilman, D. W., & Hunt, S. J. (2010). Global peatland dynamics since the last glacial maximum. *Geophysical Research Letters*, *37*(13), L13402. https://doi.org/10.1029/2010GL043584

Yu, Z., Vitt, D. H., & Wieder, R. K. (2014). Continental fens in western Canada as effective carbon sinks during the Holocene. *The Holocene*, *24*(9), 1090–1104. https://doi.org/10.1177/0959683614538075

Yu, Z. C. (2012). Northern peatland carbon stocks and dynamics: A review. *Biogeosciences*, *9*(10), 4071–4085. https://doi.org/10.5194/bg-9-4071-2012

Zhang, H., & Väliranta, M. (2024). To better detect drivers of peatland carbon accumulation rates and patterns. *Environmental Research Letters*, *19*(4), 041004. https://doi.org/10.1088/1748-9326/ad33d6

Zhang, H., Väliranta, M., Piilo, S., Amesbury, M. J., Aquino-López, M. A., Roland, T. P., et al. (2020). Decreased carbon accumulation feedback driven by climate-induced drying of two southern boreal bogs over recent centuries. *Global Change Biology*, *26*(4), 2435–2448. https://doi.org/10.1111/gcb.15005

Zhao, B., & Zhuang, Q. (2023). Peatlands and their carbon dynamics in northern high latitudes from 1990 to 2300: A process-based biogeochemistry model analysis. *Biogeosciences*, *20*(1), 251–270. https://doi.org/10.5194/bg-20-251-2023

Zhao, Y., Liu, C., Li, X., Ma, L., Zhai, G., & Feng, X. (2023). *Sphagnum* increases soil's sequestration capacity of mineral-associated organic carbon via activating metal oxides. *Nature Communications*, *14*(1), 5052. https://doi.org/10.1038/s41467-023-40863-0

Zoltai, S. C., & Tarnocai, C. (1975). Perennially frozen peatlands in the western Arctic and Subarctic of Canada. *Canadian Journal of Earth Sciences*, *12*(1), 28–43. https://doi.org/10.1139/e75-004